CHAPTER IV
RESULTS AND DISCUSSION

4.1 Catalyst Characterization

This section shows the effects of the amount of ceria (Ce) and zirconia (Zr) loading on the catalyst characterizations, which are the BET surface area, X-ray diffraction (XRD), temperature programmed reduction (TPR), FT-Raman spectroscopy and scanning electron microscopy (SEM).

4.1.1 BET surface area

The $Ce_{1-x}Zr_xO_2$ mixed oxide catalysts surface areas ($x = 0$, 0.25, 0.50, 0.75, 1.0) were measured by the multiple point BET method. The effects of Ce and Zr loadings and calcination temperatures on the BET surface areas of catalysts were given in Tables 4.1 and 4.2.

Table 4.1 BET surface areas of catalysts prepared with the aging time = 50 h

Calcination Temperature (°C)	BET Surface Area (m^2g^{-1})				
	Ce : Zr Ratio				
	100 : 0	75 : 25	50 : 50	25 : 75	0 : 100
500	101.60	108.42	116.00	120.14	79.03
900	4.638	9.20	12.54	21.30	12.24

Table 4.2 BET surface areas of catalysts prepared with the aging time = 120 h

Calcination Temperature (°C)	BET Surface Area (m^2g^{-1})				
	Ce : Zr Ratio				
	100 : 0	75 : 25	50 : 50	25 : 75	0 : 100
500	105.1	115.1	125.3	133.7	86.28
900	6.719	9.589	28.60	34.13	33.51

As shown in Tables 4.1 and 4.2, it is found that the BET surface areas of $Ce_{1-x}Zr_xO_2$ mixed oxide catalysts (x = 0.25, 0.50, 0.75) calcined at both 500 and 900°C are higher than that of pure CeO_2. The explanation for these results may lie with the shapes of the individual particles. The pure CeO_2 particles are mainly long thin needle shaped, whereas the zirconia doped ceria particles are long thin needle shaped, and the needles can be arranged in a spherical shape, therefore resulting in a larger surface area than a relatively smooth surfaced long thin needle shaped would have.

Moreover, when the amount of added zirconia was increased, it can be seen that the BET surface areas of the $Ce_{1-x}Zr_xO_2$ mixed oxide catalysts were increased. For an example, the samples prepared with the aging time equal to 50 h and calcined at 500°C, the BET surface area of $Ce_{0.25}Zr_{0.75}O_2$ (120.14 m^2g^{-1}) is higher than $Ce_{0.50}Zr_{0.50}O_2$ (116.00 m^2g^{-1}) and $Ce_{0.75}Zr_{0.25}O_2$ (108.42 m^2g^{-1}), respectively. This can be explained by the following explanation, the addition or incorporation of zirconia to ceria as mixed oxides can enhance the thermal stability of CeO_2, resulting in better resistance of sintering and deactivation processes. It is clear that CeO_2 undergoes a rapid crystallite growth process since the BET surface areas of both catalysts that have the aging time equal to 50 and 120 h decrease significantly more than in the $Ce_{1-x}Zr_xO_2$ mixed oxide samples (x = 0.25, 0.50, 0.75). Therefore, the crystallite growth process is retarded or disfavourd by the incorporation of Zr ions into the CeO_2 matrix. The catalysts, which the aging time equal to 120 h,

have larger BET surface areas than those of 50 h do. Since, the spherical shape of the particles that arranged from the needles occurred in the function of the aging time.

From Tables 4.1 and 4.2, the results show that even the $Ce_{1-x}Zr_xO_2$ mixed oxide catalysts were calcined at high temperature (900°C), their BET surface areas were still larger than the catalysts prepared by other conventional methods. These results support for the hypothesis, which the catalysts prepared by the sol-gel technique can have a higher surface area compared to the conventional techniques. On the basis of the same reactants, for the examples, from the BET surface area of the mixed oxides prepared by the co-precipitation method, which was studied by Rossignol *et al.* (1999). For the mixed oxides calcined at 500°C, the BET surface areas of $Ce_{1-x}Zr_xO_2$, which $x = 0$, 0.25, 0.50 and 1.0, were 47, 53, 44 and 36, respectively.

BET surface areas of the catalysts calcined at 900°C were smaller than those calcined at 500°C. Since, a sintering of catalyst was occurred at high temperature resulted in a decreasing surface area.

4.1.2 X-ray Diffraction (XRD)

The XRD patterns of samples with different Ce and Zr loadings are given in Figures 4.1 and 4.2 for the samples calcined at 500°C and Figures 4.3 and 4.4 for the samples calcined at 900°C with the varying aging time.

For the $Ce_{1-x}Zr_xO_2$ mixed oxide catalysts that have the aging time equal to 50 and 120 h and calcined at 500°C, as can be seen in Figures 4.1 and 4.2, there are two XRD patterns, which are $Ce_{0.50}Zr_{0.50}O_2$ and $Ce_{0.75}Zr_{0.25}O_2$ mixed oxide catalysts, that similar to the XRD pattern of CeO_2 alone.

The XRD pattern of $Ce_{0.50}Zr_{0.50}O_2$ mixed oxide catalyst shown the six main reflections typical of a fluorite-structured material with a fcc cell, corresponding to the (111), (200), (220), (311), (222) and (400) planes (at

about 29°, 33°, 48°, 56°, 60°and 70°, (2θ)). There was some tetragonality of the obtained phase as suggested by the splitting of the (111), (200) and (220) reflection at about 30°, 35° and 50°(2θ), respectively.

For $Ce_{0.75}Zr_{0.25}O_2$ mixed oxide catalyst, the six main reflections typical of a fluorite-structured material with a fcc cell also be observed.

$Ce_{1-x}Zr_xO_2$ preferably crystallizes into a cubic structure if x is equal or lower than 0.50, whereas a tetragonal cell is preferred for x is higher than 0.50.

Note that after calcination at 500°C, the sample XRD pattern both had the aging time equal to 50 and 120 h (Figures 4.1 and 4.2) shown no evidence for extra peaks due to nonincorporated ZrO_2 was found in any XRD spectrum, suggesting that ZrO_2 was incorporated into the CeO_2 lattice to form a solid solution while maintain the fluorite structure.

The XRD patterns of $Ce_{1-x}Zr_xO_2$ mixed oxide catalysts that have the aging time equal to 50 and 120 h and calcined at 900°C are shown in Figures 4.3 and 4.4. The positions of XRD peaks (2θ) of the sample calcined at 500 and 900°C are almost the same, but the peak intensity of the sample calcined at 900°C is higher than the sample calcined at 500°C. The different intensity of the peaks may originate from the different degree of porosity and crystallinity of CeO_2 and ceria-zirconia.
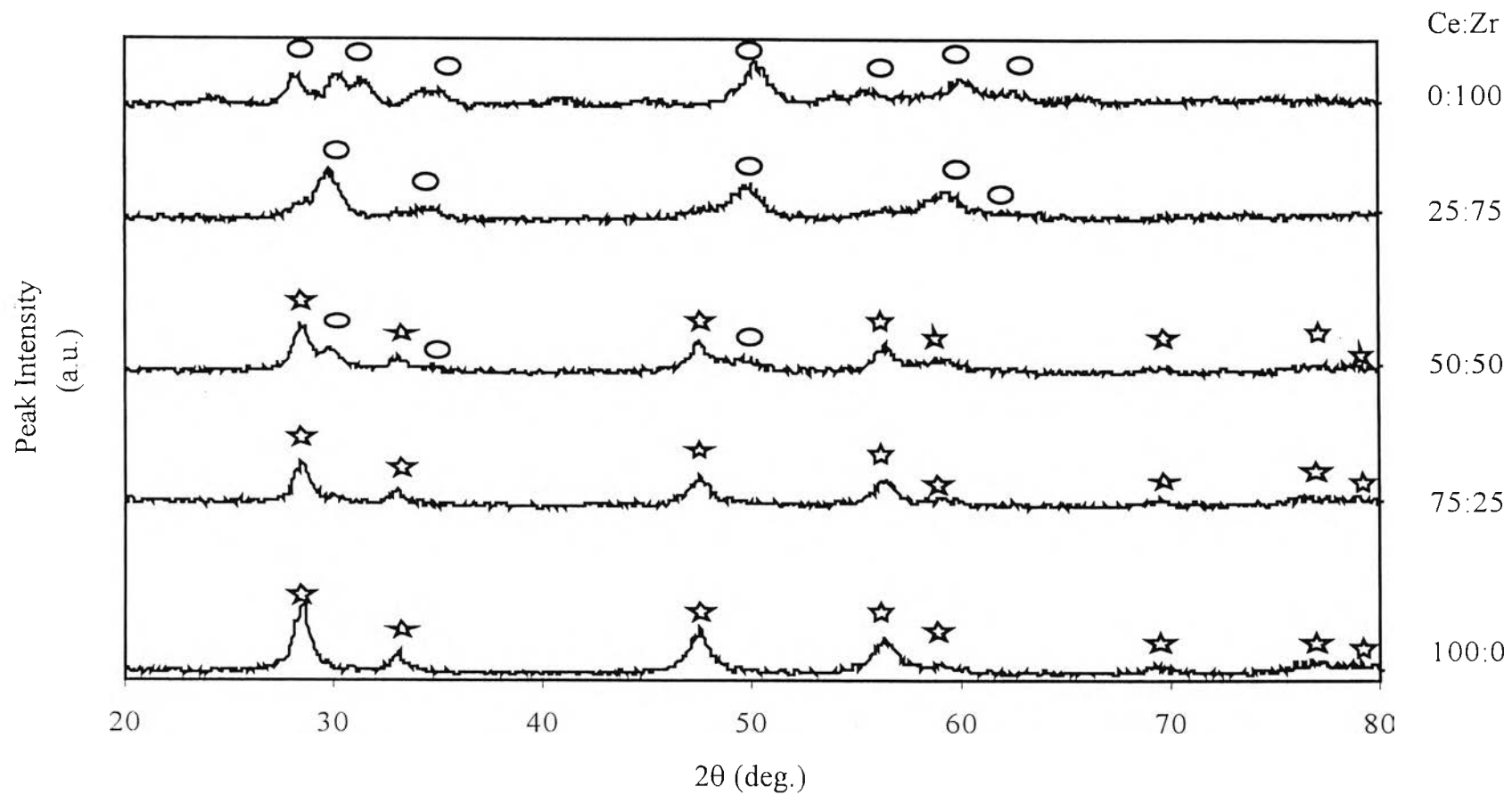
Figure 4.1 XRD patterns for $Ce_{1-x}Zr_xO_2$ mixed oxide catalysts with the aging time = 50 h and calcined at 500°C: (o) tetragonal phase; (☆) cubic phase
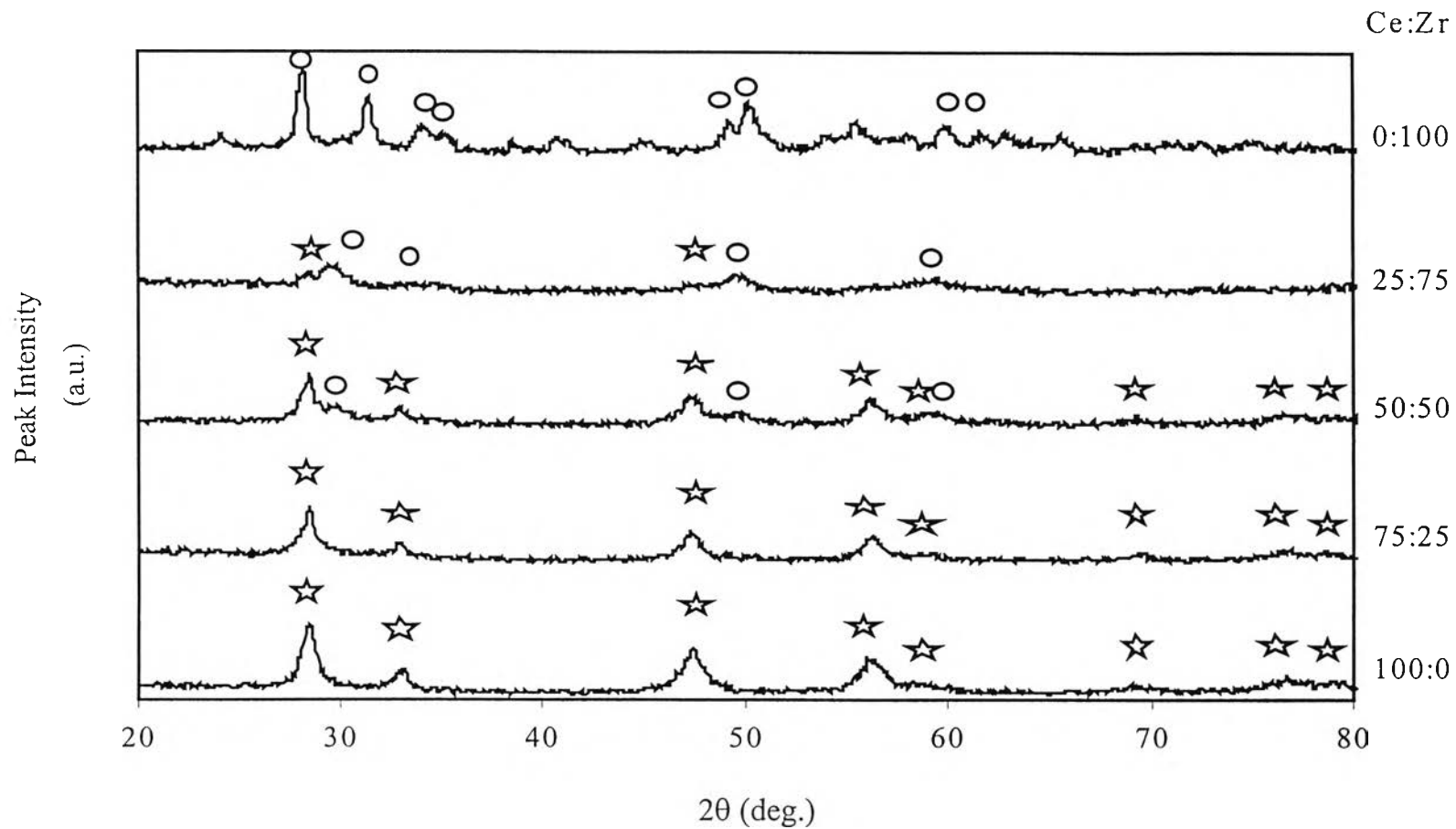
Figure 4.2 XRD patterns for $Ce_{1-x}Zr_xO_2$ mixed oxide catalysts with the aging time = 120 h and calcined at 500°C: (o) tetragonal phase; (☆) cubic phase

The XRD pattern of CeO_2 alone is assigned to be a fluorite-cubic phase. The XRD patterns that similar to CeO_2 are observed in $Ce_{0.50}Zr_{0.50}O_2$ and $Ce_{0.75}Zr_{0.25}O_2$ mixed oxide catalysts.

The XRD pattern of $Ce_{0.50}Zr_{0.50}O_2$ mixed oxide catalyst shown the six main reflections typical of a fluorite-structured material with a fcc cell, corresponding to the (111), (200), (220), (311), (222) and (400) planes (at about 29°, 33°, 48°, 56°, 60°and 70°, (2θ)). There was some tetragonality of the obtained phase as suggested by the splitting of the (111), (220) and (222) reflection at about 30°, 50° and 60°(2θ), respectively.

For $Ce_{0.75}Zr_{0.25}O_2$ mixed oxide catalyst, the six main reflections typical of a fluorite-structured material with a fcc cell also be observed.
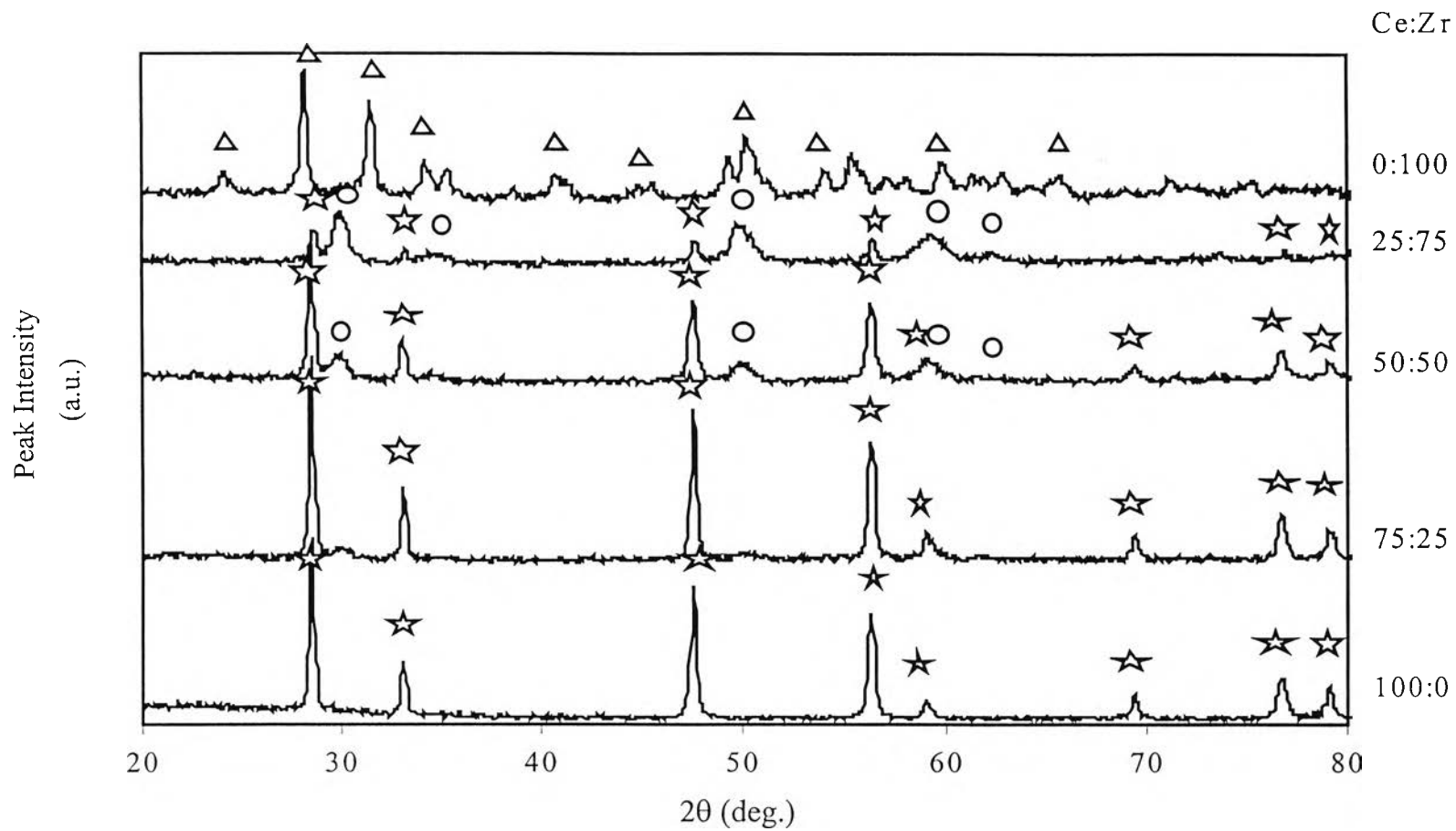
For the samples calcined at 900°C, $Ce_{1-x}Zr_xO_2$ preferably crystallizes into a cubic structure if x is equal or lower than 0.50, whereas a tetragonal cell is preferred for x is higher than 0.50, and a monoclinic phase is observed at the higher ZrO_2 content.

As can be seen in Figures 4.1 to 4.4 that the characteristic of the patterns of ZrO_2 alone were not observed in any of the samples, which had varying ratios of ceria to zirconia ($x = 0.25$, 0.50 and 0.75). These suggesting that ZrO_2 be incorporated into the CeO_2 lattice to form a solid solution while maintain the fluorite structure.
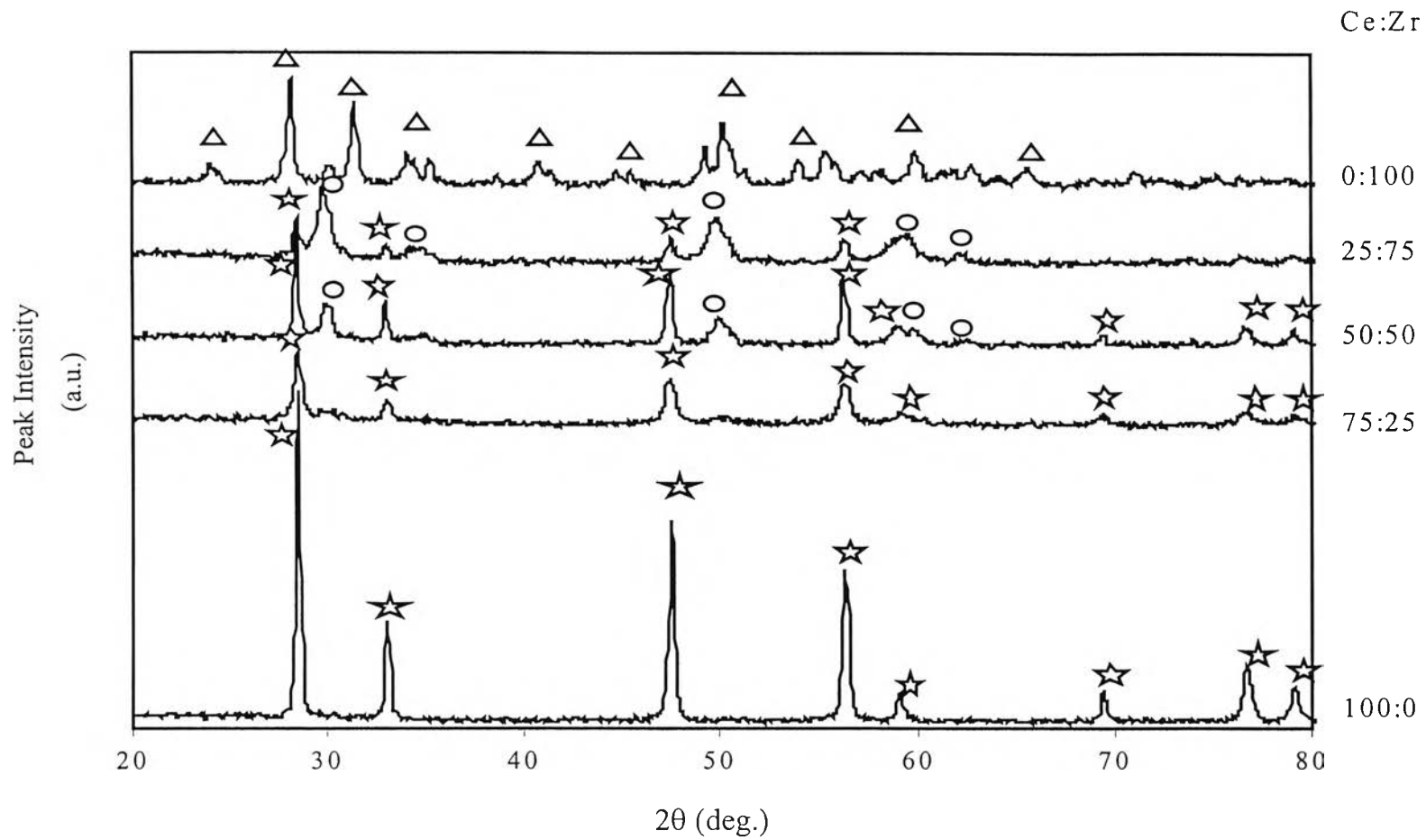
Figure 4.3 XRD patterns for $Ce_{1-x}Zr_xO_2$ mixed oxide catalysts with the aging time = 50 h and calcined at 900^oC: (o) tetragonal phase; (☆) cubic phase

Figure 4.4 XRD patterns for $Ce_{1-x}Zr_xO_2$ mixed oxide catalysts with the aging time = 120 h and calcined at 900°C: (o) tetragonal phase; (☆) cubic phase

A tetragonal cell deriving from a cubic cell with a slight displacement of oxygen anion from their ideal fluorite sites has been also observed at composition of x is equal or lower than 0.50. This phase is generally referred as a cubic phase because its XRD pattern is indexed in the cubic Fm3m space group. The presence of a cubic-only phase in $Ce_{0.75}Zr_{0.25}O_2$ mixed oxide catalysts is in agreement with the above observations and also indicates that Ce and Zr are homogeneously distributed (the presence of Ce- or Zr-rich domains would lead to preferential formation of more than one phase).

From Figures 4.1 to 4.4, the diffraction peaks observed are shifted to higher degrees with a rise in the amount of Zr incorporated to CeO_2. This observation indicates a shrinkage of the lattice due to the replacement of Ce^{4+} with Zr^{4+}, which coincides with the fact that the cation radius of Zr^{4+} (r (Zr^{4+}) = 0.86 Å) is lower that that of Ce^{4+} (r(Ce^{4+}) = 1.09 Å). As compared with the XRD spectrum of CeO_2 alone, XRD peaks observed for the $Ce_{1-x}Zr_xO_2$ solid solution became broader (x = 0.25, 0.50 and 0.75). This broadening could be ascribed to the distortion of cubic phase of fluorite structure to a tetragonal one, which due to the incorporation of Zr into CeO_2.

The lack of free ZrO_2 was also confirmed by FT-Raman spectroscopy.

4.1.3 Temperature Programmed Reduction (TPR)

The reactivity of lattice oxygen in $Ce_{1-x}Zr_xO_2$ mixed oxide catalysts (x = 0, 0.25, 0.50, 0.75 and 1.0) towards H_2 was investigated by TPR technique. Figures 4.5 and 4.6 show the TPR profiles as a function of temperature obtained for the $Ce_{1-x}Zr_xO_2$ mixed oxide catalysts calcined at 500°C while Figures 4.7 and 4.8 show the TPR profiles for the samples calcined at 900°C with the varying aging time.

Two peaks with maxima at 507-665°C and 663-827°C, respectively, were observed for most of the samples. The relative intensities of all peaks strongly depended on CeO_2 content.

All peaks were associated with the reduction of the $Ce_{1-x}Zr_xO_2$ mixed oxide catalysts. In Figure 4.5, for CeO_2 alone, the main peak for H_2 consumption was observed at approximately 805°C. In addition to this peak, a weak peak was observed ca. 514°C. Two peaks were also investigated for CeO_2 alone in Figure 4.6, which were observed at 801 and 508°C. These two peaks were also reported in other studies and were interpreted to correspond with the reduction of the bulk oxygen and the easily reducible surface oxygen, respectively. In contrast with CeO_2, only very small amount of H_2 was consumed for ZrO_2 up to 1000°C because its structure was monoclinic, which almost irreducible.
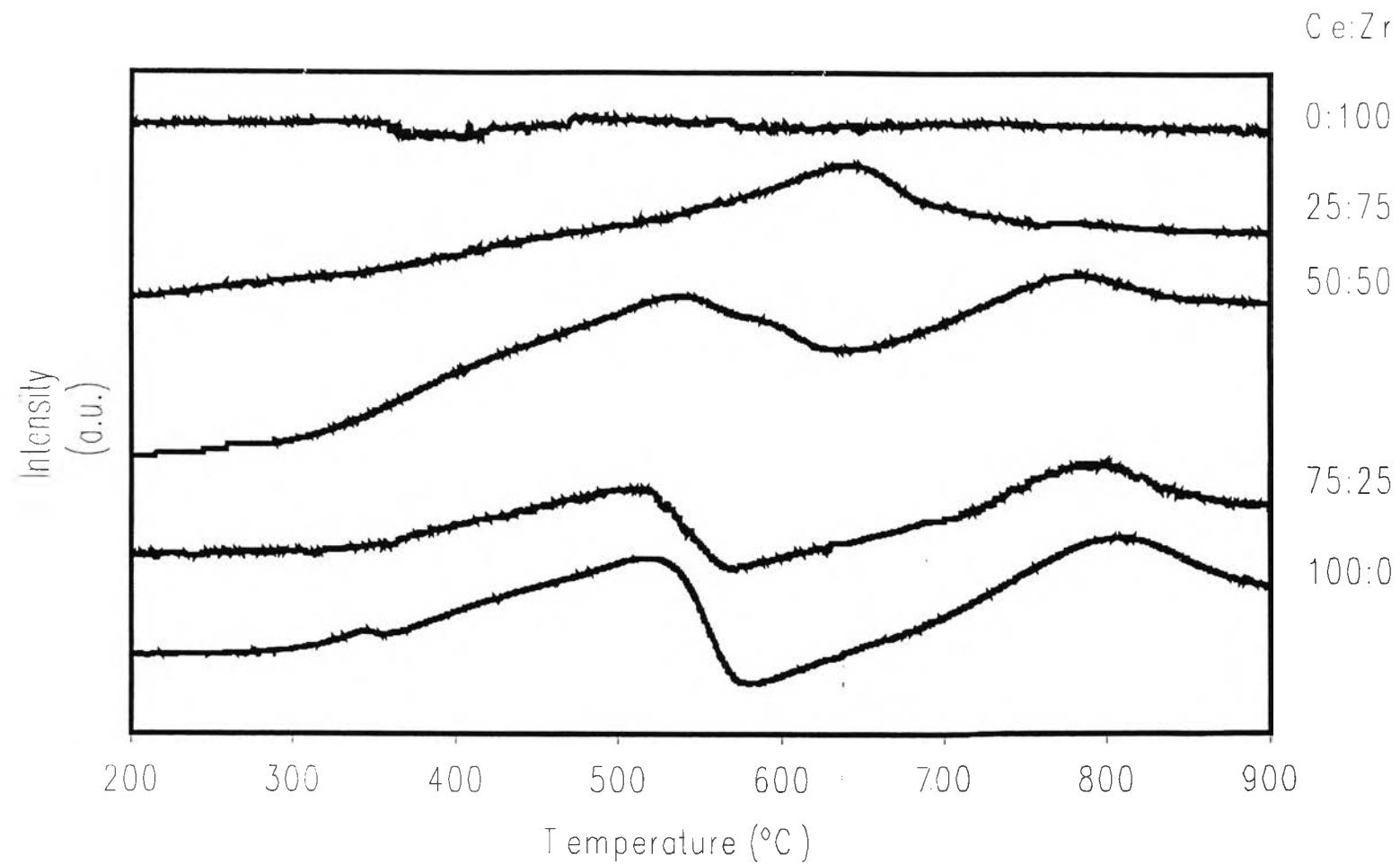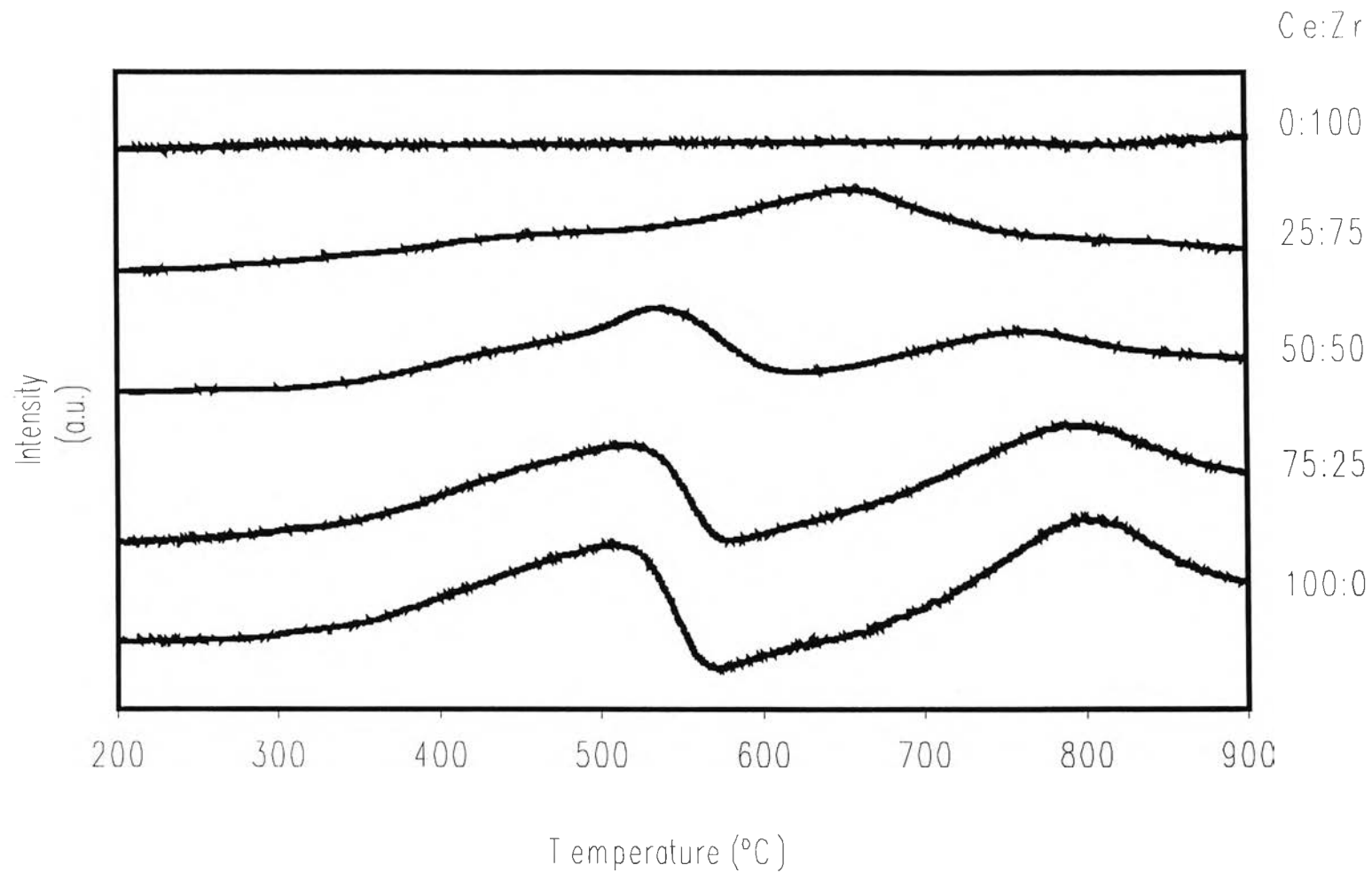
Figure 4.5 TPR profiles of $Ce_{1-x}Zr_xO_2$ mixed oxide catalysts with the aging time = 50 h and calcined at 500°C

Figure 4.6 TPR profiles of $Ce_{1-x}Zr_xO_2$ mixed oxide catalysts with the aging time = 120 h and calcined at 500°C

There was a very strong promotion of the reducibility of the $Ce_{1-x}Zr_xO_2$ mixed oxide catalysts as shown by the appearance of a peak at 507-665°C (Henceforth, the feature at 507-665°C will be indicated as the LT, viz. Low temperature, peak and the feature at 663-827°C as the HT, viz. High temperature, peak.). Accordingly, the LT and HT features have to be associated with the reduction of the bulk solid solutions.

It should be noted that the temperature of the maximum of the LT peak strongly depends on the nature of the sample. It decreases on decreasing the cerium molar content from 100 to 75 mol %, while further decrease from 50 to 25 mol % broadens and shifts the LT peak to higher temperatures. All HT peaks, however, shifted to lower temperatures. Although similar to that for CeO_2 alone, two peaks were observed for $Ce_{0.75}Zr_{0.25}O_2$ and $Ce_{0.50}Zr_{0.50}O_2$; the peak at the low temperature region (507-665°C) became the major one. Obviously, such a peak could not be ascribed only to the reduction of the surface oxygen, because the dominant H_2 consumption of the low temperature peaks. The reduction of the bulk lattice oxygen in the solid solution becomes easier because of the distortion of the structure, which caused by the partial substitution of Ce^{4+} with Zr^{4+} in the sol-gel technique. As a result, reduction of the bulk lattice oxygen must occur simultaneously with the reduction of surface oxygen.

The relative intensities of all peaks strongly depend on CeO_2 content. The intensity of the high temperature peak is negligible for $Ce_{0.25}Zr_{0.75}O_2$ in both catalysts that have the aging time equal to 50 and 120 h, and calcined at 500°C, resulting in only one main peak. This is caused from the influence of the irreducible monoclinic form of the larger amount of zirconium ion added compare to cerium ion.

Figures 4.7 and 4.8 show the TPR profiles as a function of temperature obtained for the $Ce_{1-x}Zr_xO_2$ mixed oxide catalysts calcined at 900°C with the aging time equal to 50 and 120 h, respectively.

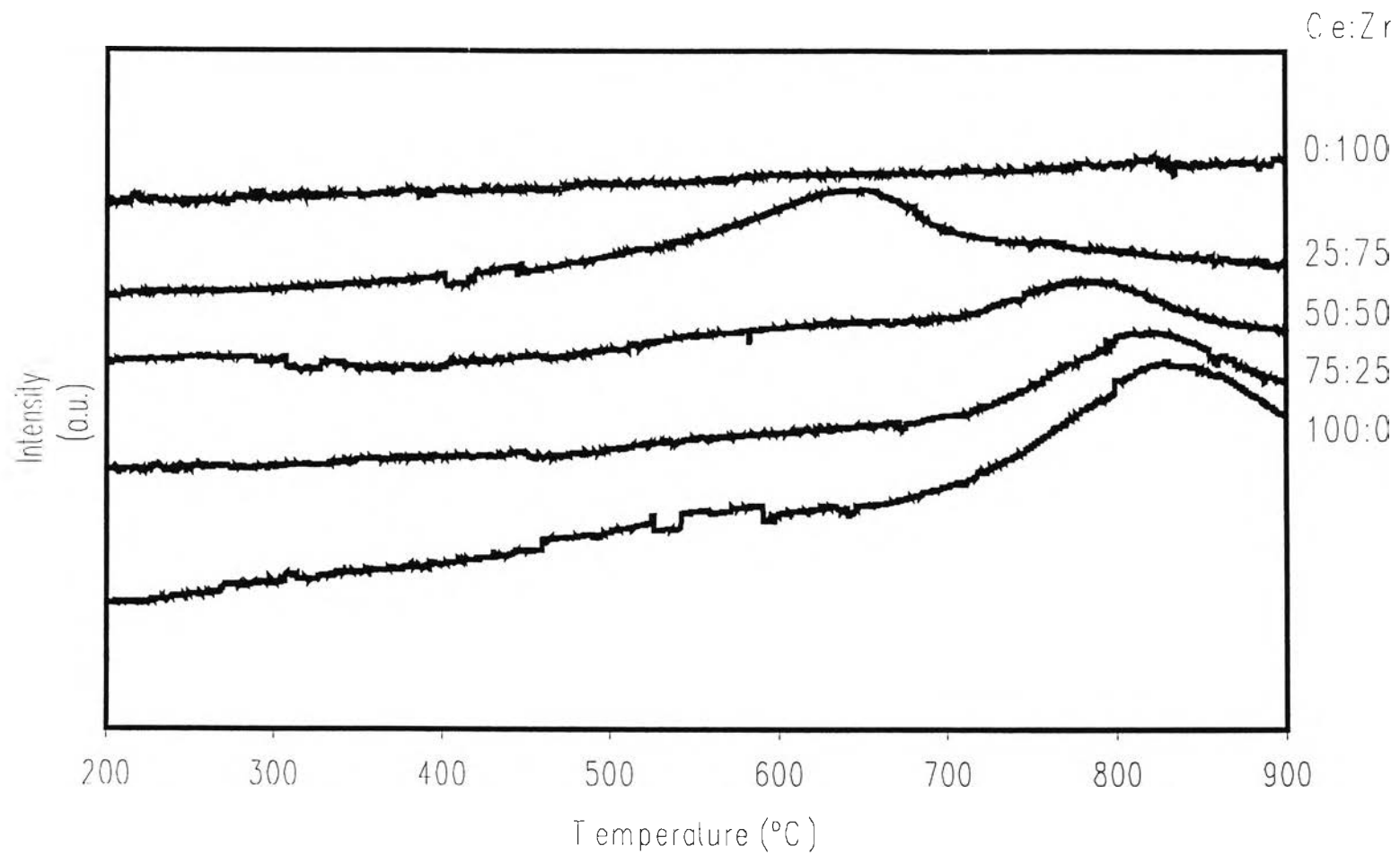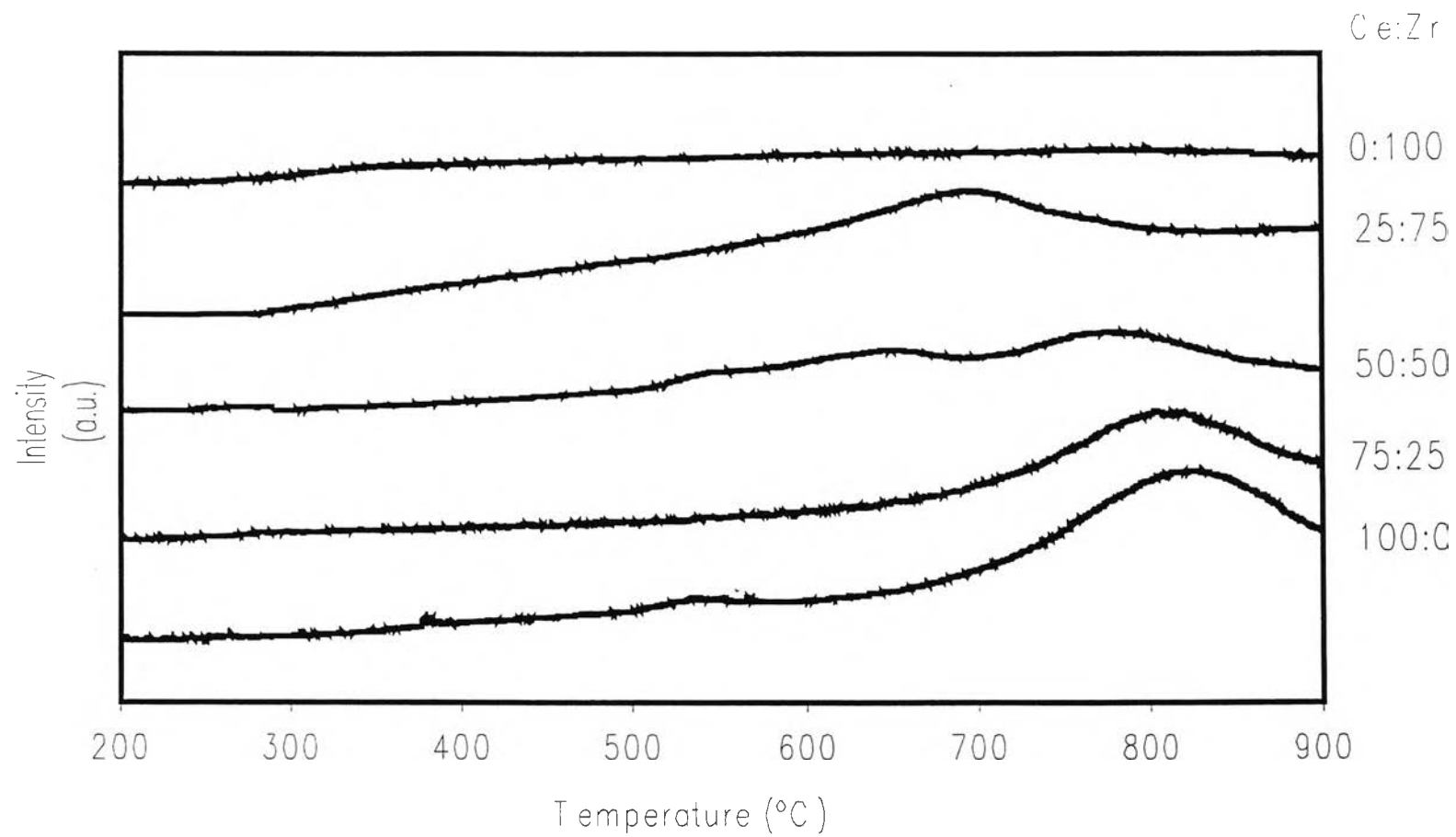**Figure 4.7** TPR profiles of $Ce_{1-x}Zr_xO_2$ mixed oxide catalysts with the aging time = 50 h and calcined at 900°C

Figure 4.8 TPR profiles of $Ce_{1-x}Zr_xO_2$ mixed oxide catalysts with the aging time = 120 h and calcined at 900°C

The reactivity of lattice oxygen in $Ce_{1-x}Zr_xO_2$ mixed oxide catalysts toward H_2 was investigated by TPR technique. For the $Ce_{1-x}Zr_xO_2$ mixed oxide catalysts that had the aging time equal to 50 and 120 h, and calcined at $900°C$, the low temperatures were almost disappeared for all ratios of ceria to zirconia ($x = 0$, 0.25, 0.50 and 0.75). Since the surface areas were reduced from the calcination at high temperature ($900°C$). As a result, the low temperature peaks, which were mainly caused by the reduction of surface oxygen, became the minor peaks compared to those that calcined at $500°C$.

The TPR patterns shown in Figures 4.7 and 4.8 of $Ce_{1-x}Zr_xO_2$ mixed oxide catalysts calcined at $900°C$ indicate that the increasing amount of zirconium molar content results in decreasing the reduction temperature.

The summary of the results of the TPR experiments carried out on all the samples having the aging time of 50 h and 120 h are reported in Table 4.3 and Table 4.4, respectively.

Table 4.3 TPR results of catalysts prepared with the aging time = 50 h

Ce : Zr Ratios	Peak temperatures for catalyst reduction ($°C$)			
	Calcination Temperatures ($°C$)			
	500		900	
	LT	HT	LT	HT
100 : 0	514	805	*	827
75 : 25	507	791	*	820
50 : 50	536	773	*	786
25 : 75	642	*	*	663
0 : 100	*	*	*	*

* No peak was observed

Table 4.4 TPR results of catalysts prepared with the aging time = 120 h

Ce : Zr Ratios	Peak temperatures for catalyst reduction (°C)			
	Calcination Temperatures (°C)			
	500		900	
	LT	HT	LT	HT
100 : 0	508	801	535	821
75 : 25	512	793	*	804
50 : 50	531	763	665	772
25 : 75	654	*	*	691
0 : 100	*	*	*	*

* No peak was observed

Some interesting features immediately appear from a perusal of Tables 4.3 and 4.4: formation of a solid solution between ceria and zirconia, which strongly promotes the reduction of the mixed oxide catalysts as a new reduction feature with a maximum below 665°C, is observed. The splitting of the support reduction process into two peaks clearly depends on CeO_2 content. The data reported in Tables 4.3 and 4.4 clearly suggest an optimal range of composition is 75 % of CeO_2 for obtaining a reduction at low temperatures (507-512°C). Notably, the LT peak shifts toward higher temperatures on decreasing the CeO_2 content. Similarly for CeO_2 ⟨ 75%, the LT peak also shifts toward higher temperatures.

In summary, it clearly appears form the TPR results that there is an optimum ratio of composition (x = 0.25) where the lowest reduction temperatures are observed and that in the cubic structure the reduction process is kinetically favoured compared to the tetragonal one.

These results have the similar trends to those of the Fornasiero *et al.* (1995) and Otsuka *et al.* (1999).

4.1.4 FT-Raman Spectroscopy

Figures 4.9 to 4.12 show the FT-Raman spectra of $Ce_{1-x}Zr_xO_2$ mixed oxide catalysts (x = 0, 0.25, 0.50, 0.75 and 1.0) in the wavelength range of 400 to 900 cm^{-1}.
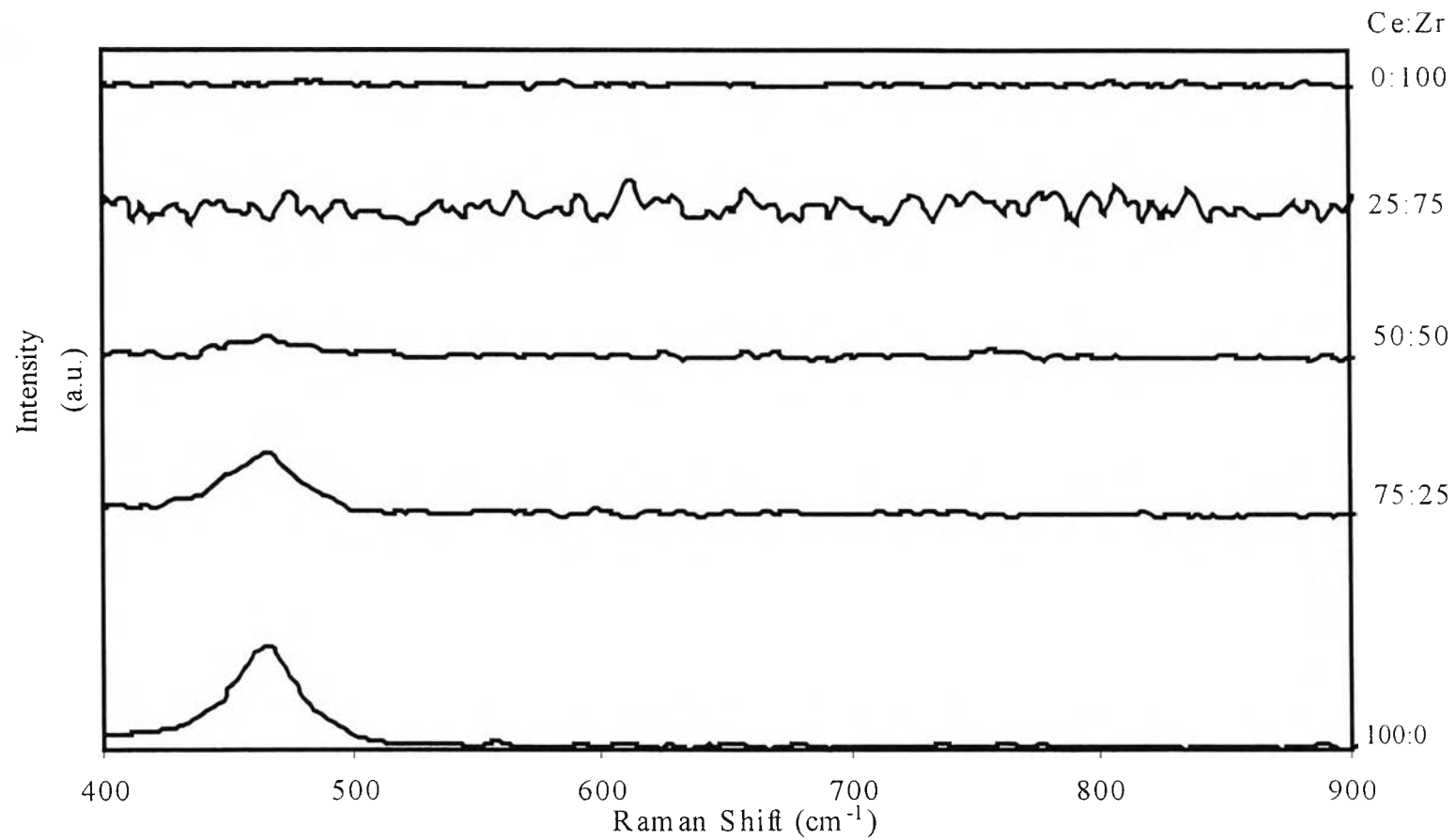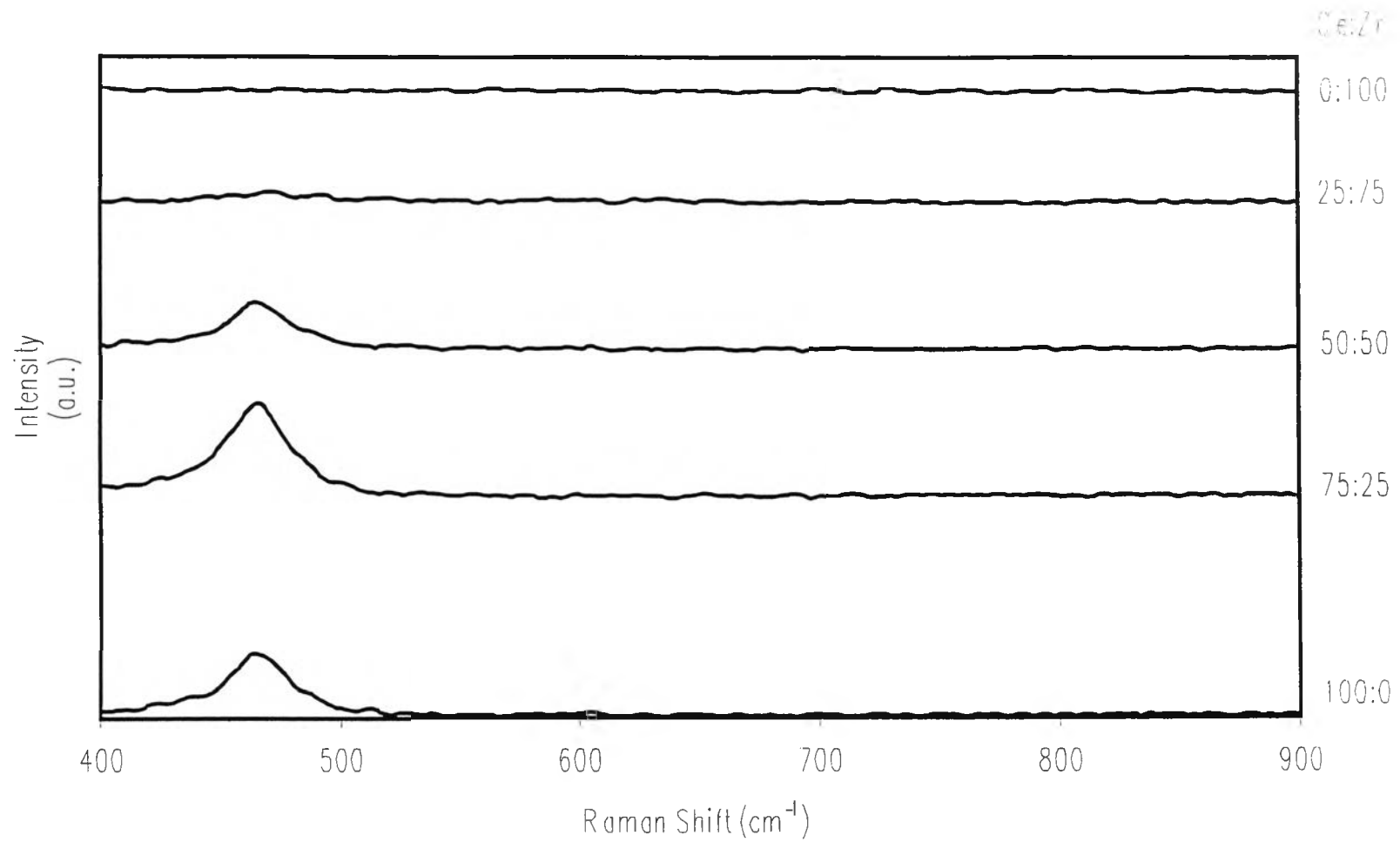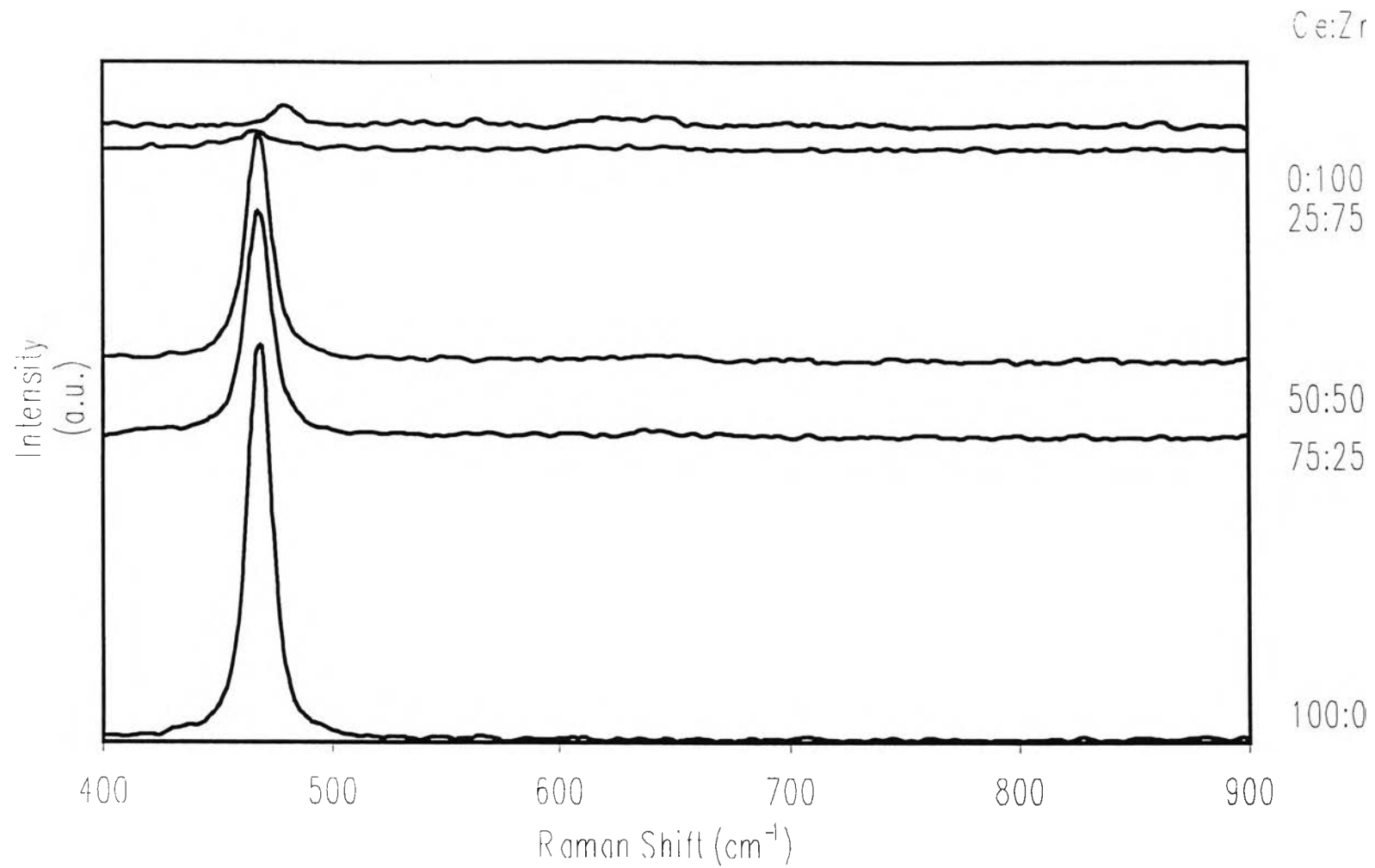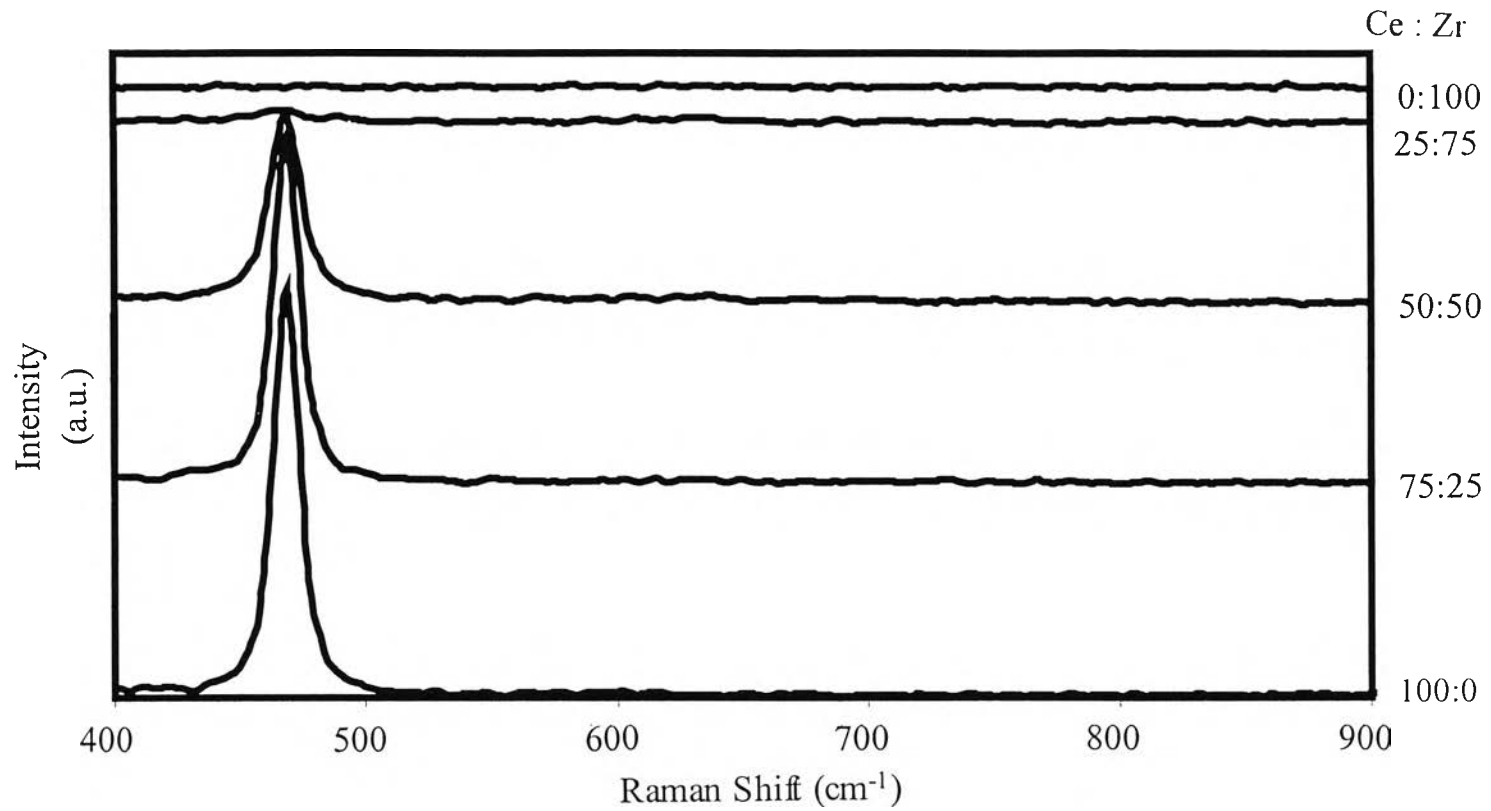
Figure 4.9 FT-Raman spectra of $Ce_{1-x}Zr_xO_2$ mixed oxide catalysts with the aging time = 50 h and calcined at $500°C$

Figure 4.10 FT-Raman spectra of $Ce_{1-x}Zr_xO_2$ mixed oxide catalysts with the aging time = 120 h and calcined at 500°C

Figure 4.11 FT-Raman spectra of $Ce_{1-x}Zr_xO_2$ mixed oxide catalysts with the aging time = 50 h and calcined at 900°C

Figure 4.12 FT-Raman spectra of $Ce_{1-x}Zr_xO_2$ mixed oxide catalysts with the aging time = 120 h and calcined at $900^{\circ}C$

The summary of the results of the FT-Raman experiments carried out on all the samples are reported in Table 4.5 for the sample that calcined at 500°C, and Table 4.6 for the sample that calcined at 900°C.

Table 4.5 Raman shift of strong peaks of FT-Raman spectra of $Ce_{1-x}Zr_xO_2$ mixed oxide catalysts calcined at 500°C

Aging Time (h)	Raman Shift (cm^{-1})				
	Ce : Zr Ratio				
	100 : 0	75 : 25	50 : 50	25 : 75	0 : 100
50	465.0	465.0	465.0	*	*
120	463.0	465.0	465.0	*	*

* No peak was observed

Table 4.6 Raman shift of strong peaks of FT-Raman spectra of $Ce_{1-x}Zr_xO_2$ mixed oxide catalysts calcined at 900°C

Aging Time (h)	Raman Shift (cm^{-1})				
	Ce : Zr Ratio				
	100 : 0	75 : 25	50 : 50	25 : 75	0 : 100
50	466.9	463.0	465.0	465.0	478.5
120	466.9	466.9	466.9	468.8	*

The Raman spectra of both the mixed oxide catalysts, which had the aging time equal to 50 and 120 h, appear very similar: those that calcined at $500^{\circ}C$ exhibited a strong peak at about 465 cm^{-1} as shown in Figures 4.9 and Figure 4.10. The only one strong adsorption peak centered at 465 cm^{-1} typical of the F_{2g} Raman active mode of a fluorite-structured material. The patterns suggested some distortion of the oxygen lattice, which was consistent with the presence of cubic phases.

After calcination at $900^{\circ}C$, the intensity of the F_{2g} mode for the samples was increased, which shown in Figures 4.11and 4.12. This is consistent with a sample sintering, which apparently leads to a relatively ordered situation of the oxygen polyhedra around the cations (Vidal *et al.* (1999) and Daniela *et al.* (1998)). The different intensity of the band in the samples may originate from the different degree of porosity and crystallinity of CeO_2 and ceria-zirconia. No bands characteristic of pure ZrO_2 were detected, suggesting there was a partial substitution of Ce^{4+} with Zr^{4+} in the lattice of ceria.

### 4.1.5 Scanning Electron Microscopy (SEM)

Figures 4.13 to 4.20 show the morphology of the $Ce_{1-x}Zr_xO_2$ mixed oxide catalysts (x = 0, 0.25, 0.50, 0.75 and 1.0), which were the not calcined samples, the samples calcined at $500^{\circ}C$ and the samples calcined at $900^{\circ}C$, obtained by Scanning Electron Microscopy (SEM).

The particle shapes of CeO_2 alone are mainly long thin needles shaped, whereas $Ce_{1-x}Zr_xO_2$ mixed oxide catalysts, which x = 0.25, 0.50 and 0.75, the particle shapes are long thin needles shaped, and the needles can be arranged in a spherical shaped. The particle shapes of ZrO_2 are mainly the thick sheets, which look like books. Therefore, the $Ce_{0.75}Zr_{0.25}O_2$, $Ce_{0.50}Zr_{0.50}O_2$ and $Ce_{0.25}Zr_{0.75}O_2$ mixed oxide catalysts, have a higher BET surface area than CeO_2 alone.
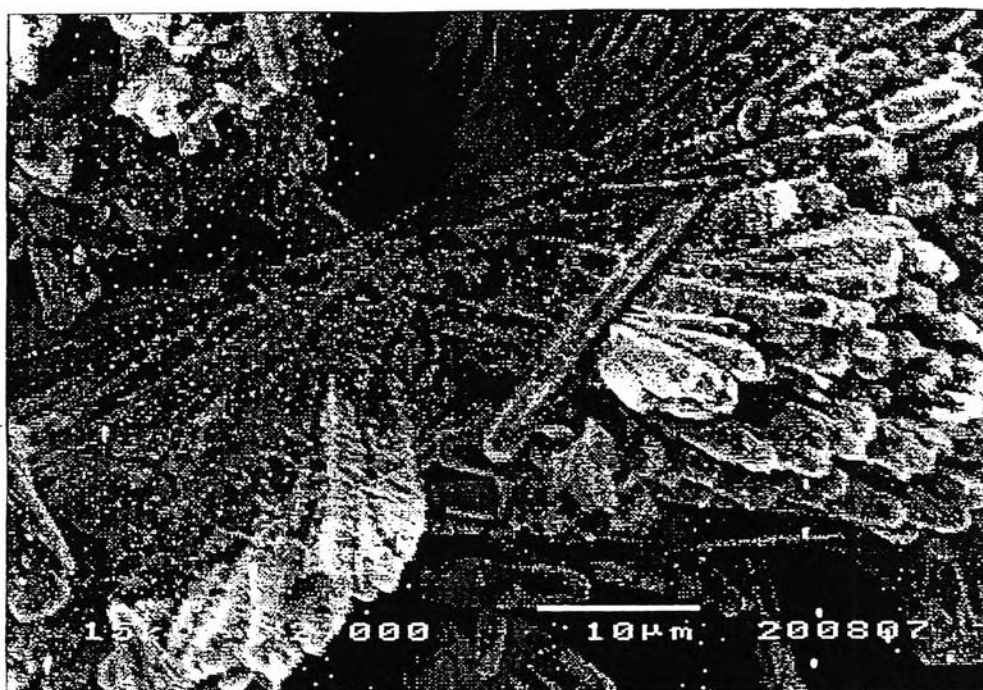
(a)
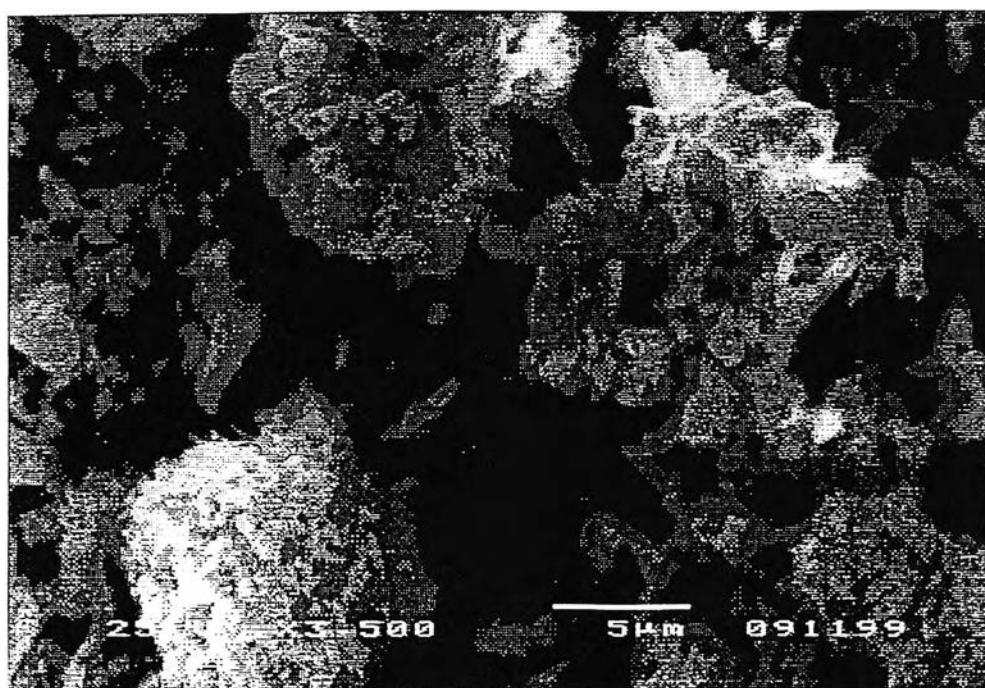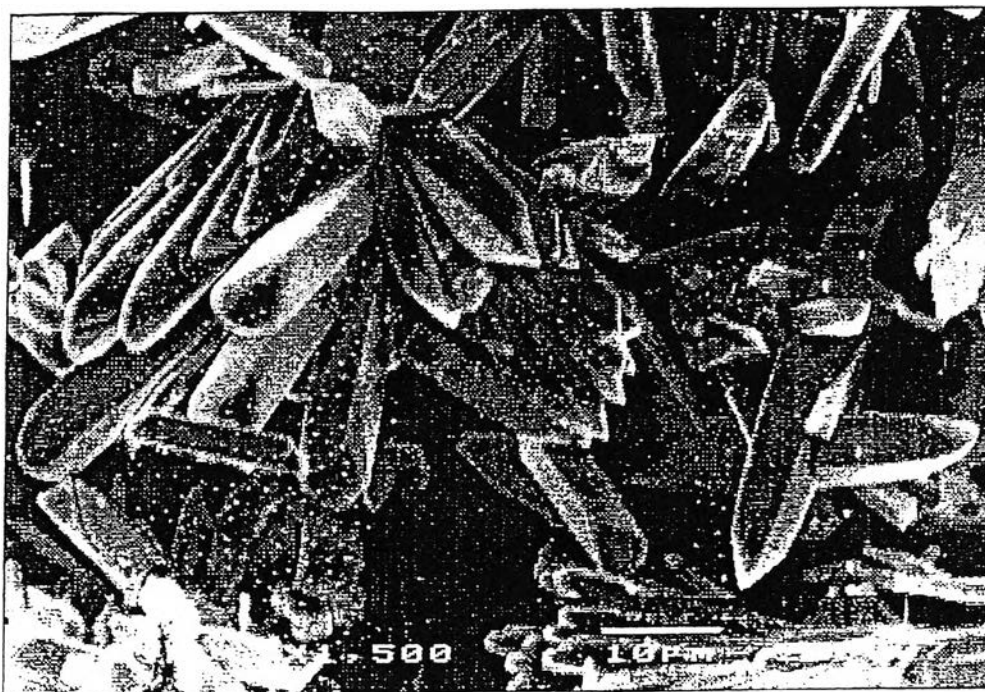

(b)

Figure 4.13 SEM pictures of not calcined CeO_2 (a) and $Ce_{0.75}Zr_{0.25}O_2$ (b) with the aging time = 50 h
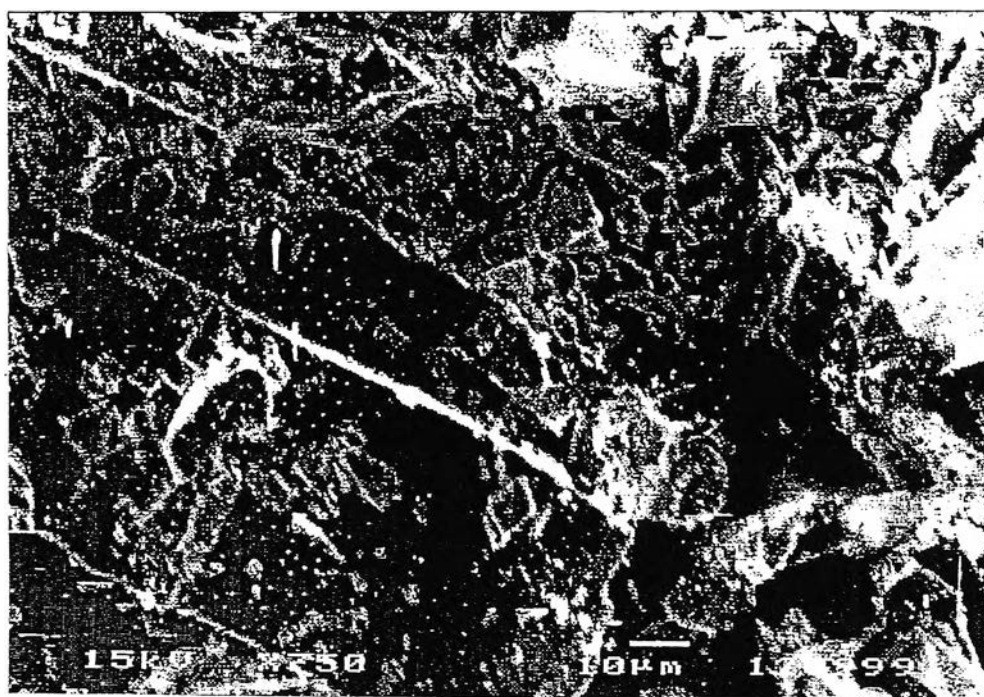
(a)

(b)

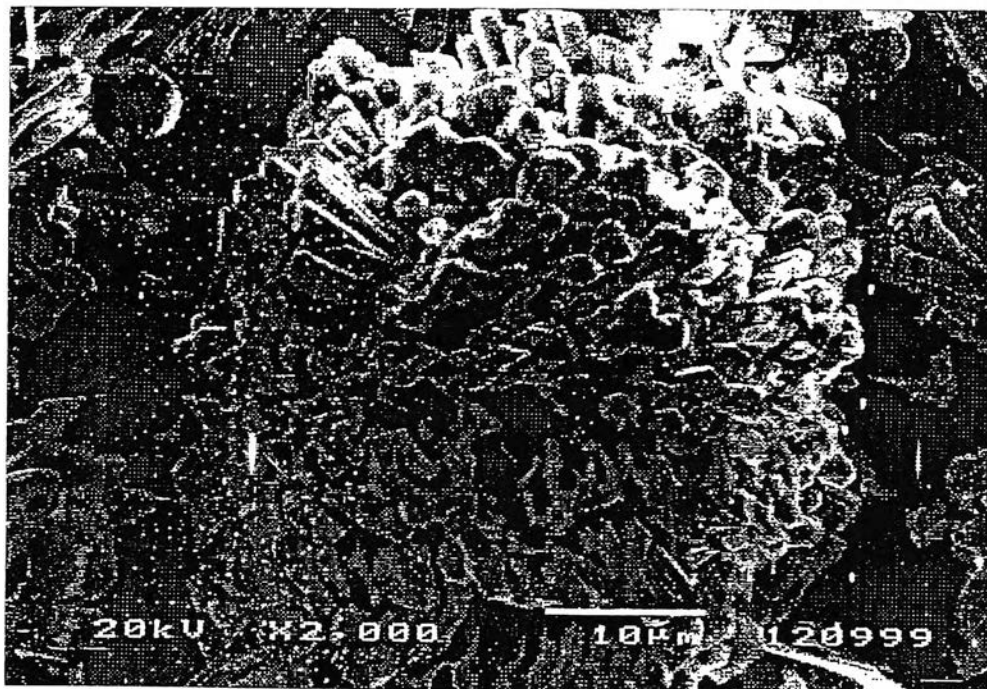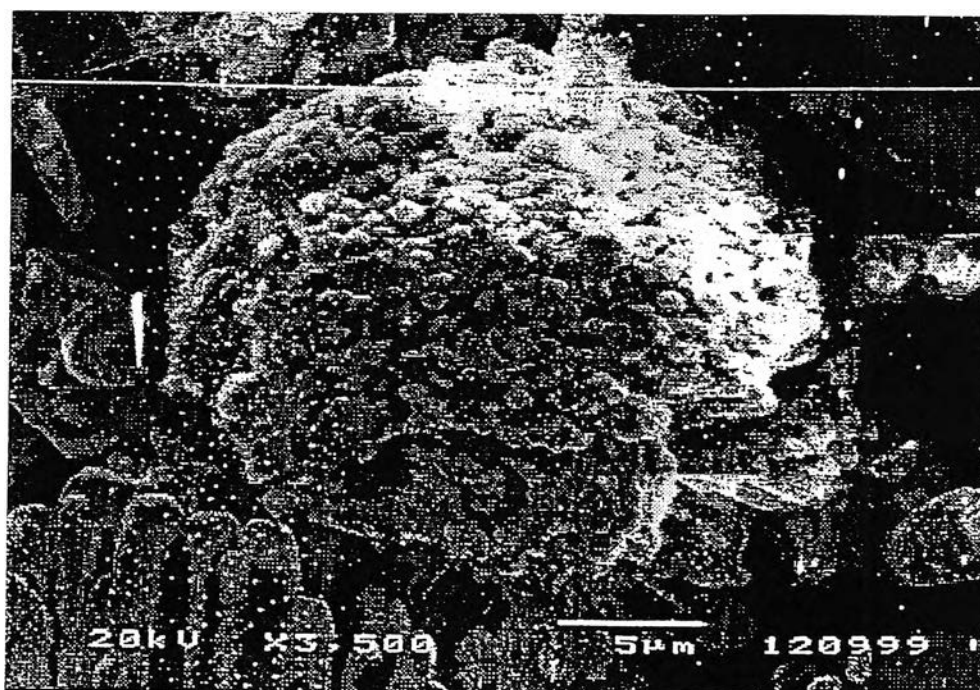**Figure 4.14** SEM pictures of not calcined $Ce_{0.50}Zr_{0.50}O_2$ (a) and $Ce_{0.25}Zr_{0.75}O_2$ (b) with the aging time = 50 h

(a)

(b)

Figure 4.15 SEM pictures of not calcined ZrO_2 (a) and CeO_2 calcined at $500^{\circ}C$ (b) with the aging time = 50 h

(a)

(b)

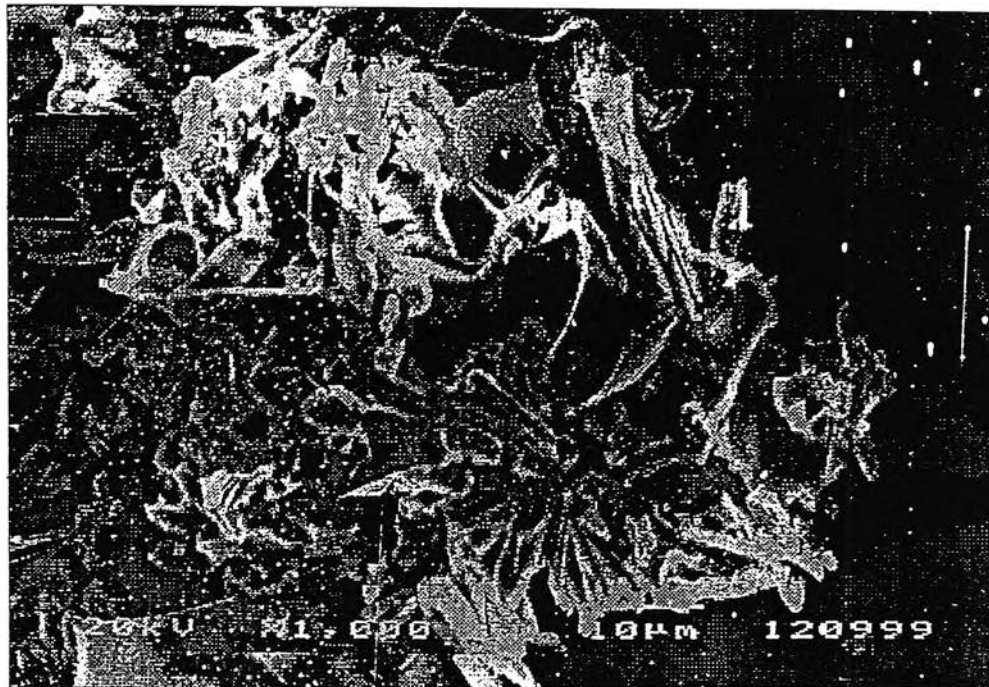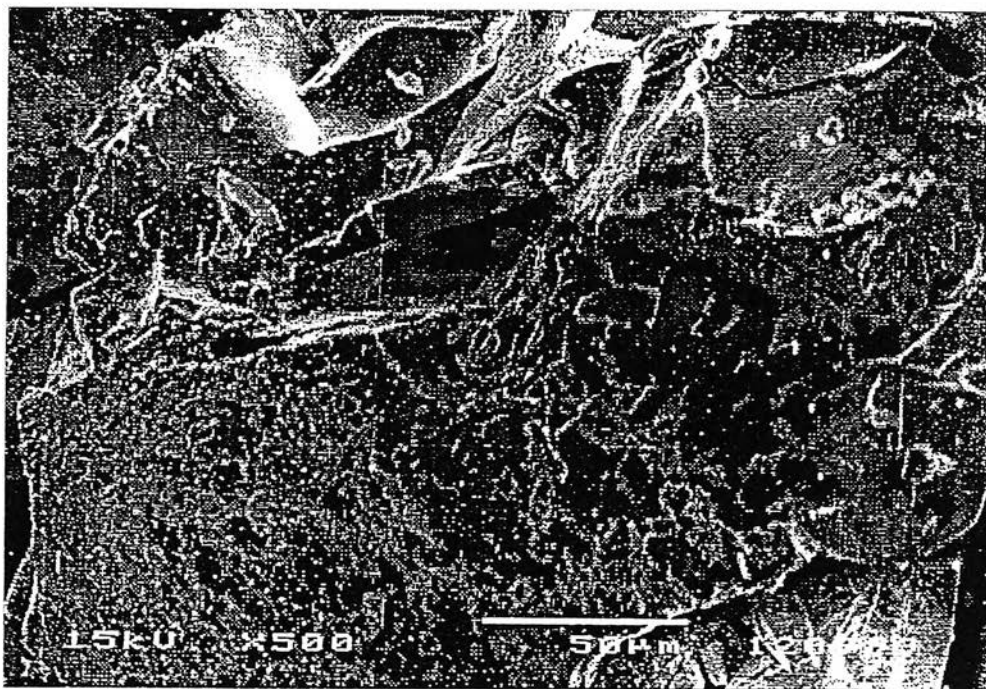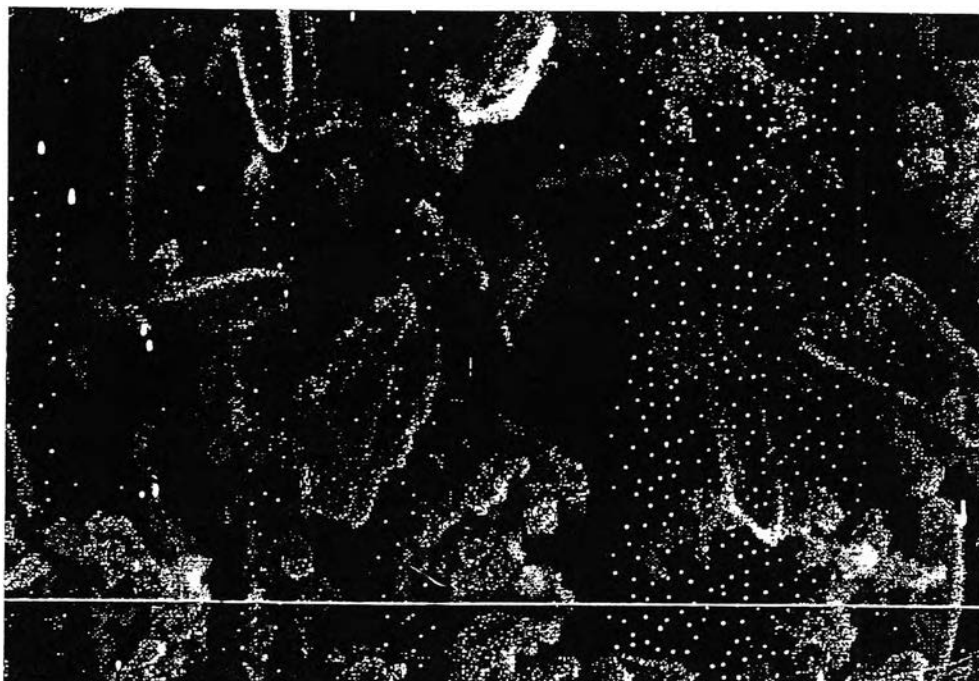**Figure 4.16** SEM pictures of $Ce_{0.75}Zr_{0.25}O_2$ (a) and $Ce_{0.50}Zr_{0.50}O_2$ (b) with the aging time = 50 h and calcined at 500^oC
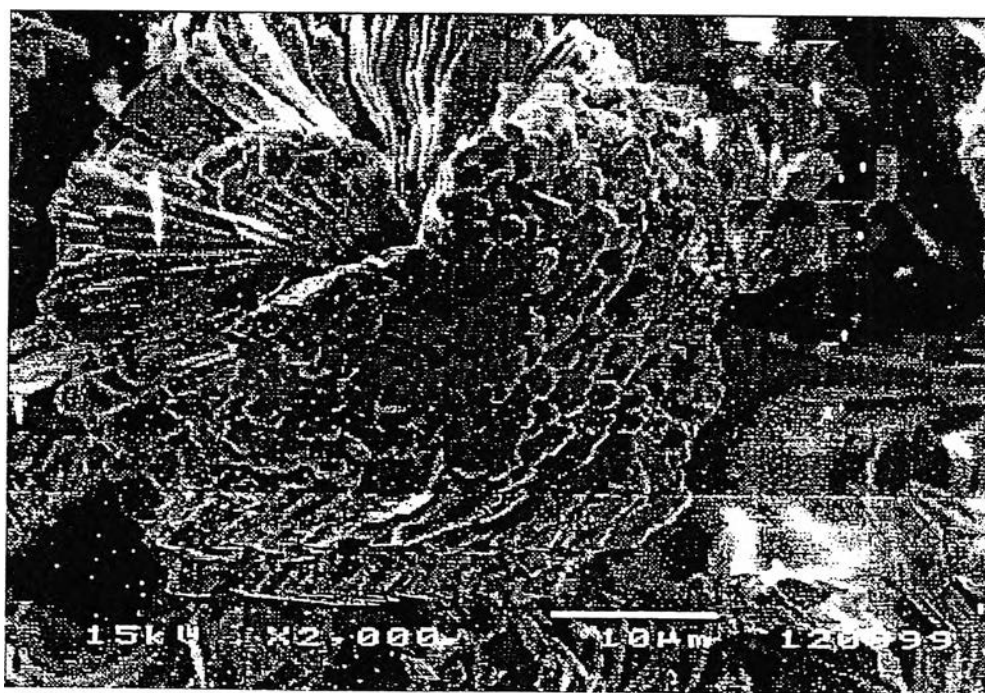
(a)

(b)

Figure 4.17 SEM pictures of $Ce_{0.25}Zr_{0.75}O_2$ (a) and ZrO_2 (b) with the aging time = 50 h and calcined at $500^{o}C$

(a)

15kU   X2,000   10μm   120999
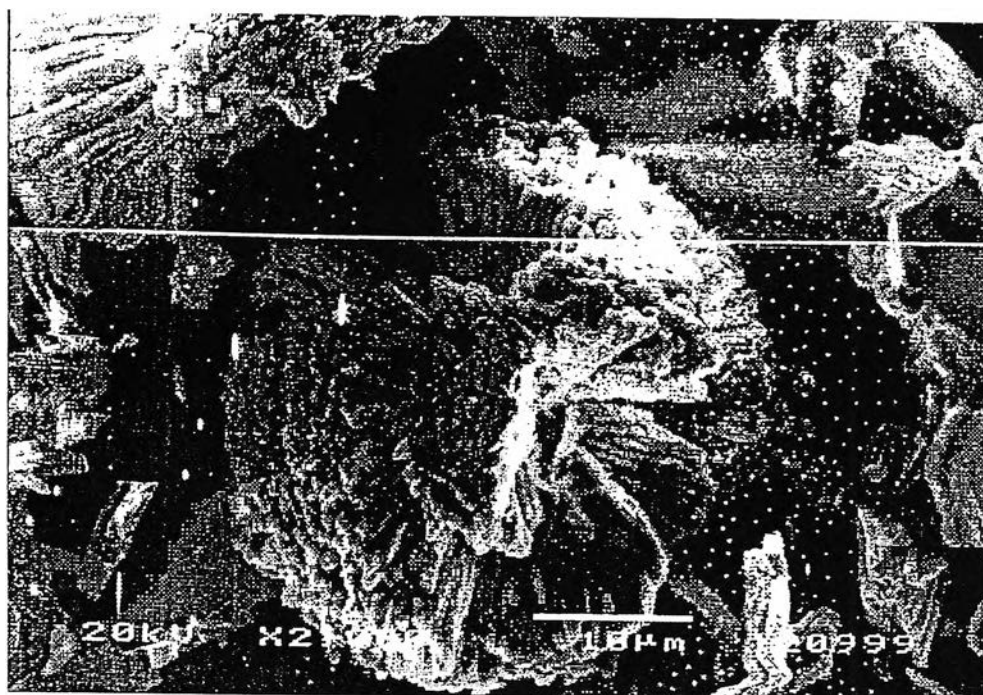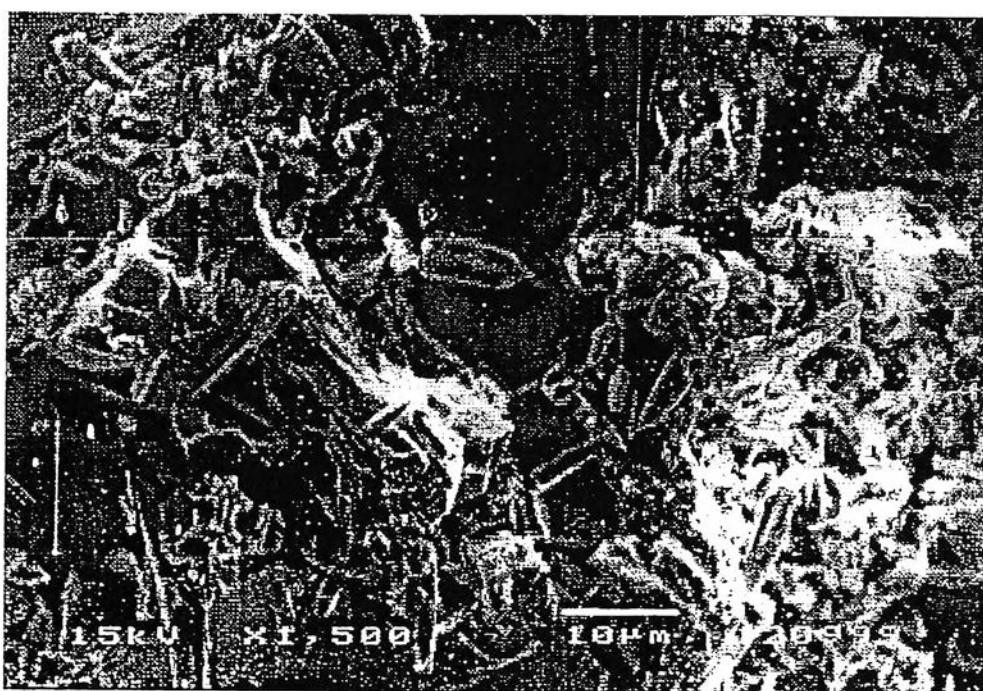
(b)

Figure 4.18 SEM pictures of CeO_2 (a) and $Ce_{0.75}Zr_{0.75}O_2$ (b) with the aging

time = 50 h and calcined at $900^{\circ}C$

(a)

(b)

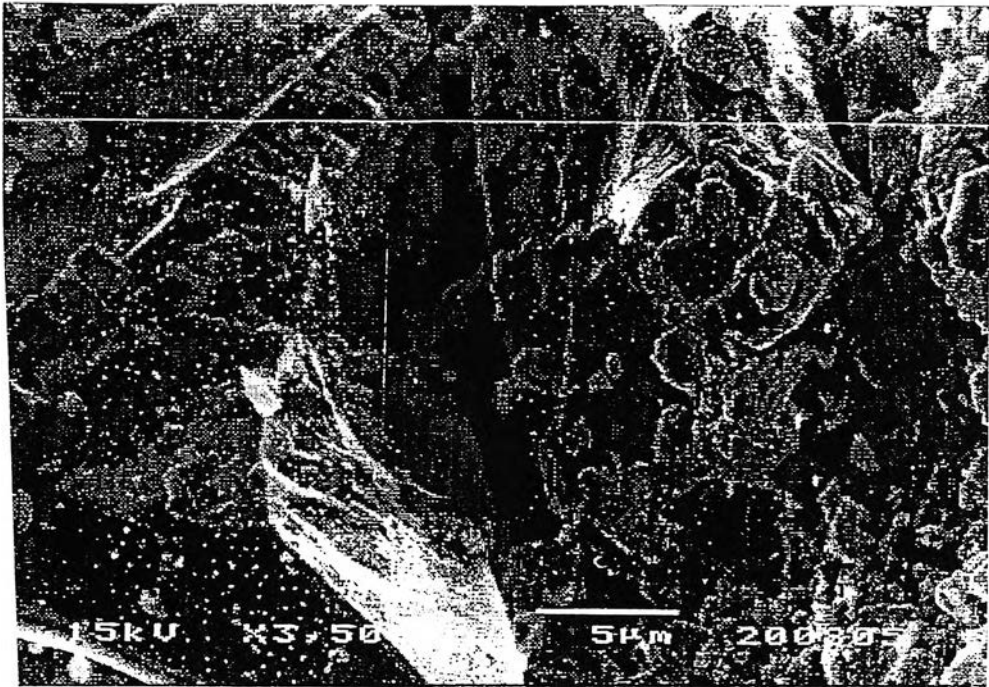**Figure 4.19** SEM pictures of $Ce_{0.50}Zr_{0.50}O_2$ (a) and $Ce_{0.25}Zr_{0.75}O_2$ (b) with the aging time = 50 h and calcined at 900°C

(a)

Figure 4.20 SEM picture of ZrO_2 with the aging time = 50 h and calcined at 900°C (a)

4.2 Activity Test

The activity of the catalyst was successfully accessed via the packed bed reactor as mentioned in section 3.2.2. Figures 4.21 to 4.25 show the light off temperature curves of the $Ce_{1-x}Zr_xO_2$ mixed oxide catalysts (x = 0.25, 0.50 and 0.75), which were tested under oxidizing and reducing conditions. The temperatures at the conversion of CO equal to 50 % (T_{50}) are tabulated from the curves shown in the Tables 4.7 to 4.10.

The reaction temperature for the light off temperature test was in the range of 200-400°C. The limitation of the temperature was caused from the glassware used, which was the Pyrex glass U-tube microreactor that cannot stand for the temperature above 400°C. The heating rate was 1°C/min. The flowrate of the total reactant gas was 50 ml/min.

The amount of catalyst used per run of reaction was about one gram.

The value of T_{50} of the catalyst can imply for its catalytic activity, which is the CO oxidation in this work. The catalyst that has lower value of T_{50} will have higher catalytic activity for CO oxidation.
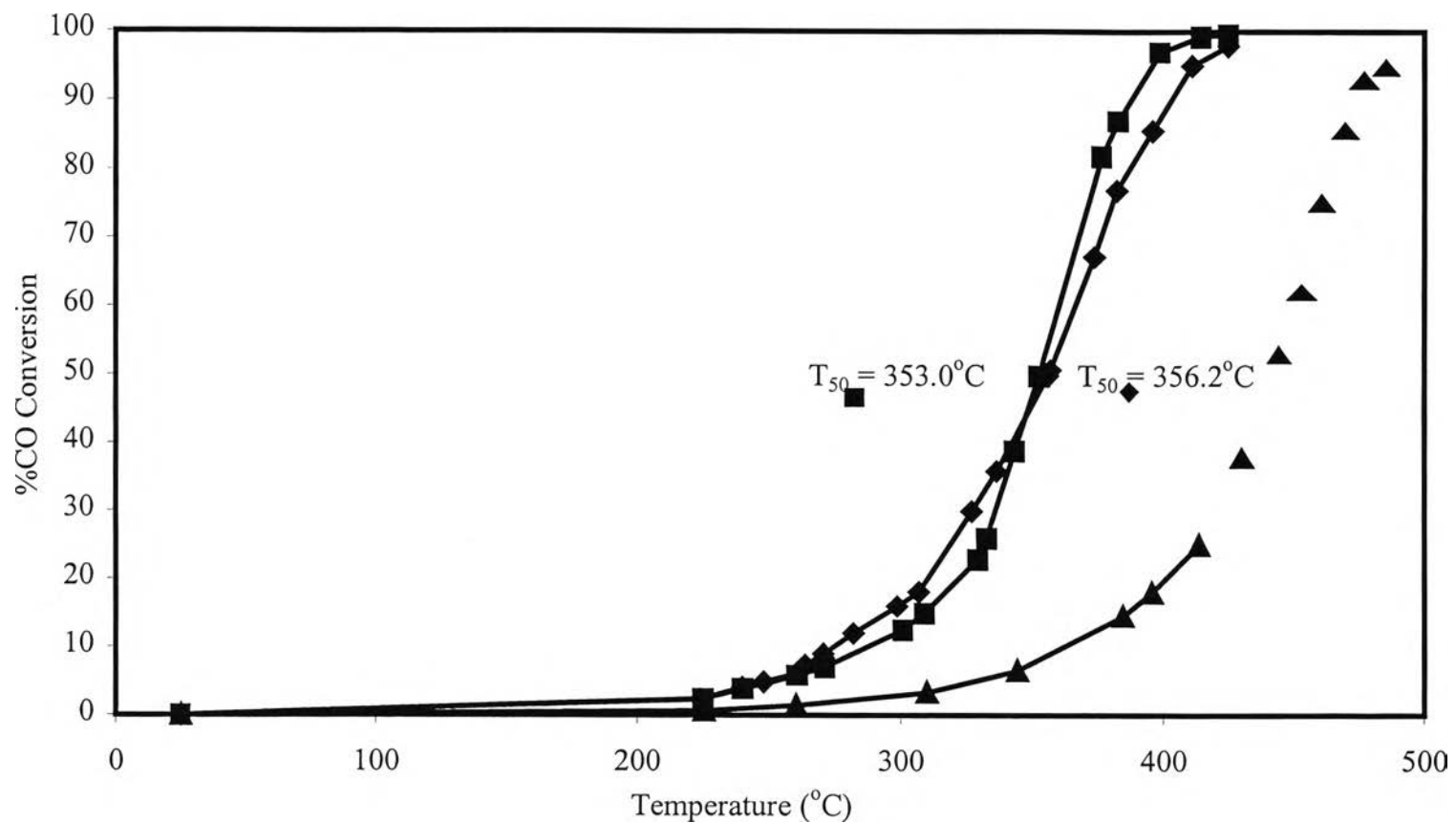
Figure 4.21 Light off temperature curves under oxidizing condition of the solid solution with the aging time = 50 h and calcined at 500°C: (♦) $Ce_{0.75}Zr_{0.25}O_2$, (■)$Ce_{0.50}Zr_{0.50}O_2$ and (▲) $Ce_{0.25}Zr_{0.75}O_2$ mixed oxide catalysts

Figure 4.21 shows the light off temperature curves of the $Ce_{1-x}Zr_xO_2$ mixed oxide catalysts for CO oxidation under oxidizing condition ($x = 0.25$, 0.50 and 0.75, respectively), which had the aging time equal to 50 h and calcined at 500°C.

The light off temperatures (T_{50}) of the $Ce_{1-x}Zr_xO_2$ mixed oxide catalysts ($x = 0.25$, 0.50 and 0.75) were compared. It was found that T_{50} of $Ce_{0.75}Zr_{0.25}O_2$ and $Ce_{0.50}Zr_{0.50}O_2$ were almost the same (353 and 356°C, respectively), and higher than T_{50} of $Ce_{0.25}Zr_{0.75}O_2$. The CO conversion of $Ce_{0.25}Zr_{0.75}O_2$ could not reached 50 % in the range of reaction temperature (200-400°C), it reach only 20 % of CO conversion at about 401°C. From the results, it can be determined that among the samples that has the aging time equal to 50 h and calcined at 500°C, the $Ce_{0.50}Zr_{0.50}O_2$ and $Ce_{0.75}Zr_{0.25}O_2$ mixed oxide catalysts have the higher catalytic activity for CO oxidation than $Ce_{0.25}Zr_{0.75}O_2$ mixed oxide catalyst.

This result can be explained by the data obtained from the catalyst characterization in this work. Firstly, from the XRD result in section 4.1.2 of these samples (Figure 4.1), it can be seen that the XRD pattern that similar to the fluorite cubic type of CeO_2 alone is observed in $Ce_{0.75}Zr_{0.25}O_2$ and $Ce_{0.50}Zr_{0.50}O_2$ mixed oxide catalysts, respectively. On the other hand, the peaks of $Ce_{0.25}Zr_{0.75}O_2$ show the characteristic of tetragonality, which caused by the increasing amount of added zirconia. It can be concluded that occurrence of the solid solution is mainly observed in $Ce_{0.75}Zr_{0.25}O_2$ and $Ce_{0.50}Zr_{0.50}O_2$ mixed oxide catalysts, respectively, and only small amount might occurred in $Ce_{0.25}Zr_{0.75}O_2$.

The Raman spectra of these samples (Figure 4.9) also support this conclusion, and in addition, it proves that $Ce_{0.25}Zr_{0.75}O_2$ is not a solid solution.

As already mentioned in the background and literature review of this work (CHAPTER II) that the solid solution can be reduced easily even at low temperature, resulted in higher conversion of CO. Therefore, $Ce_{0.75}Zr_{0.25}O_2$

and $Ce_{0.50}Zr_{0.50}O_2$ solid solutions have the higher catalytic activity for CO oxidation than $Ce_{0.25}Zr_{0.75}O_2$ mixed oxide catalyst.

Ambiguously, from their TPR results (Figure 4.5 and Table 4.3), $Ce_{0.75}Zr_{0.25}O_2$ has the reduction peak at lower temperature than $Ce_{0.50}Zr_{0.50}O_2$, thus, T_{50} of $Ce_{0.75}Zr_{0.25}O_2$ should lower than T_{50} of $Ce_{0.50}Zr_{0.50}O_2$ instead of almost the same value in this experiment (Figure 4.21). It is possible that $Ce_{0.75}Zr_{0.25}O_2$ solid solution is effected by moisture in the air resulted in its decreasing catalytic activity for CO oxidation.
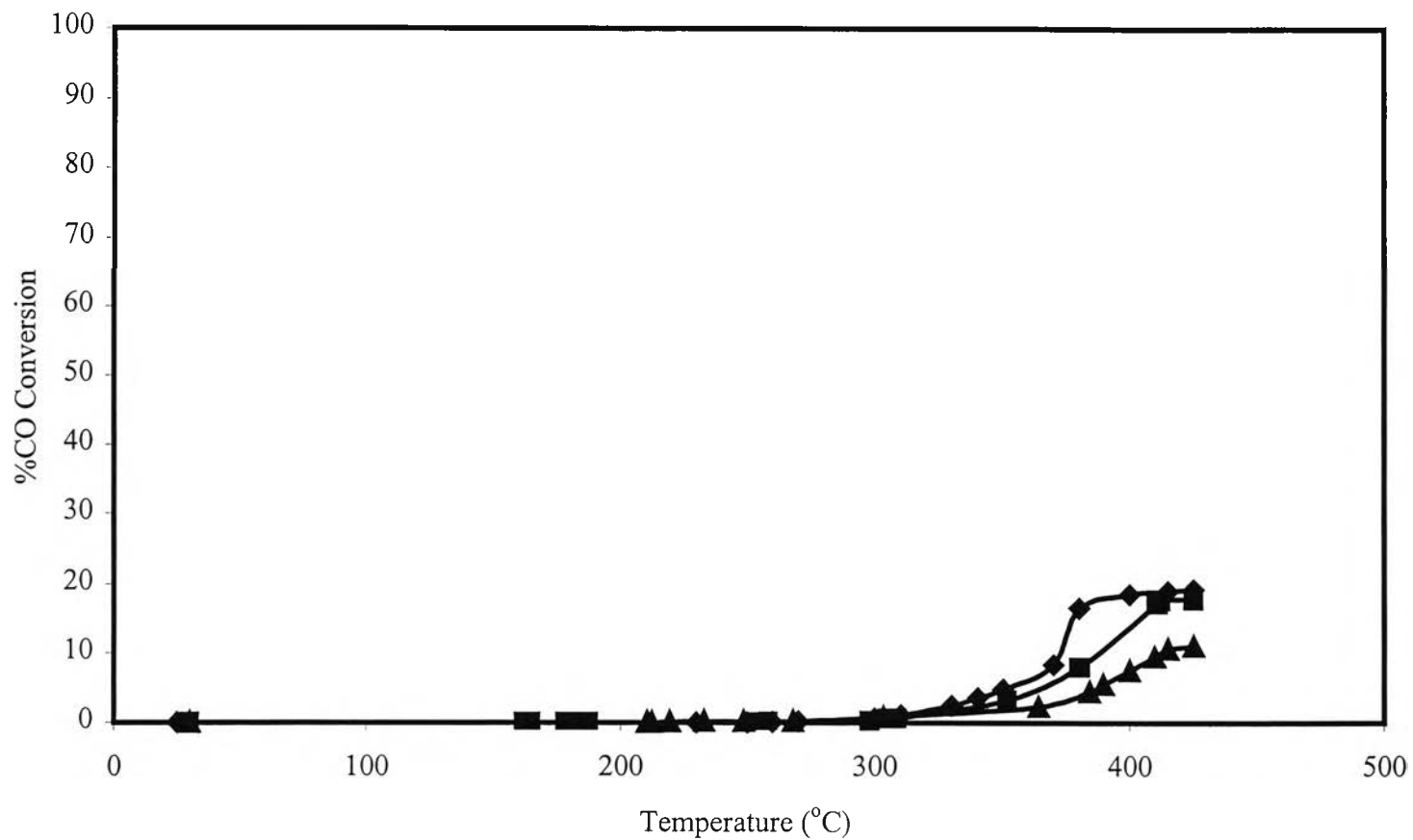
Figure 4.22 Light off temperature curves under oxidizing condition of the solid solution with the aging time = 50 h and calcined at $900^{\circ}C$: ($\blacklozenge$) $Ce_{0.75}Zr_{0.25}O_2$, ($\blacksquare$) $Ce_{0.50}Zr_{0.50}O_2$ and ($\blacktriangle$) $Ce_{0.25}Zr_{0.75}O_2$ mixed oxide catalysts

Figure 4.22 shows the light off temperature curves of $Ce_{1-x}Zr_xO_2$ mixed oxide catalysts under oxidizing condition (x = 0.25, 0.50 and 0.75), which had the aging time equal to 50 h and calcined at 900°C.

The XRD pattern (Figure 4.3) and Raman spectra (Figure 4.11) reveal that there are the observation of solid solution mostly in $Ce_{0.75}Zr_{0.25}O_2$, $Ce_{0.50}Zr_{0.50}O_2$ and $Ce_{0.25}Zr_{0.75}O_2$ mixed oxide catalysts, respectively. As a result, $Ce_{0.75}Zr_{0.25}O_2$ should have lowest T_{50}, $Ce_{0.50}Zr_{0.50}O_2$ and $Ce_{0.25}Zr_{0.75}O_2$ mixed oxide catalysts, respectively, as observed from the experiment (Figure 4.22).

From the TPR results (Figure 4.7), the low temperature peaks of that can be seen when calcined at 500°C are almost disappear, and the reductions are mainly occur at high temperature. Therefore, the catalytic activity for CO oxidation of the samples calcined at 900°C is lower than the samples calcined at 500°C. Only the samples calcined at 500°C were chosen to run the reaction further because of their better catalytic activity.
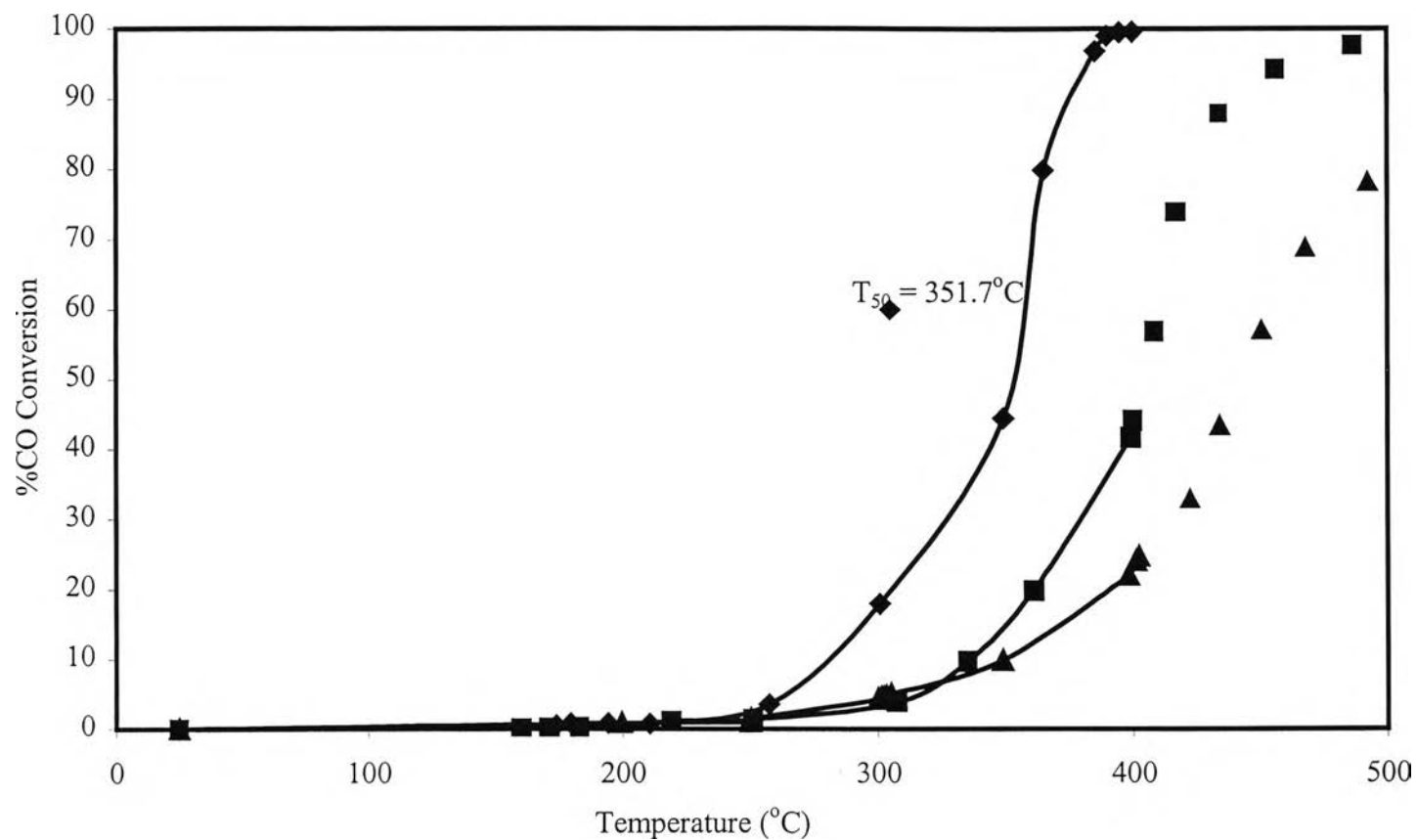
Figure 4.23 Light off temperature curves under oxidizing condition of the solid solution with the aging time = 120 h and calcined at 500°C: (♦) $Ce_{0.75}Zr_{0.25}O_2$, (■) $Ce_{0.50}Zr_{0.50}O_2$, and (▲) $Ce_{0.25}Zr_{0.75}O_2$ mixed oxide catalysts
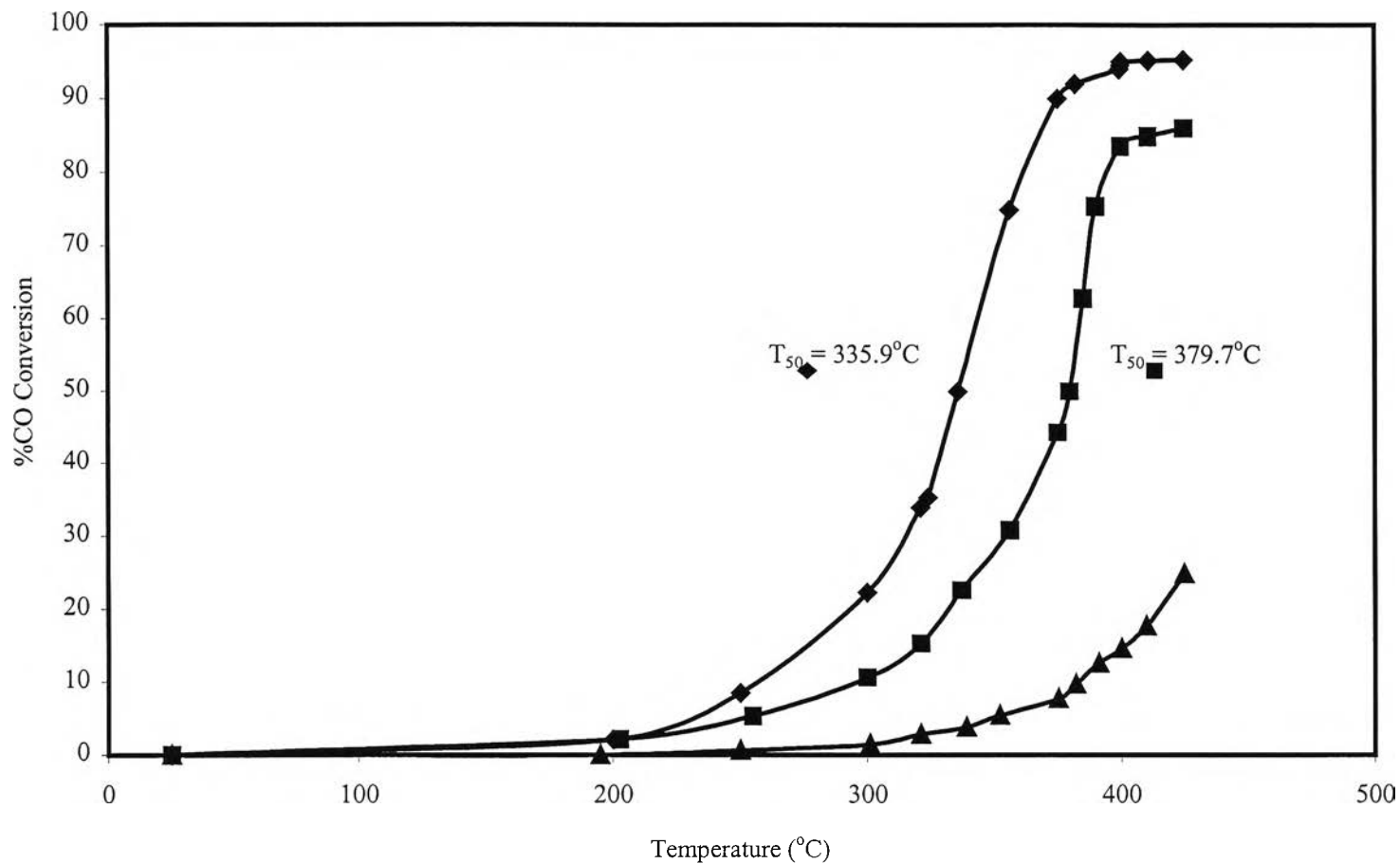
Figure 4.23 shows the light off temperature curves of the catalysts, which the aging time = 120 h and calcined at 500°C that tested under oxidizing condition. The $Ce_{0.75}Zr_{0.25}O_2$ mixed oxide catalyst has the lowest value of T_{50} (350°C) compared to $Ce_{0.50}Zr_{0.50}O_2$ (T_{50} = 410°C) and $Ce_{0.25}Zr_{0.75}O_2$ mixed oxide catalyst (T_{50} = 440°C by estimation). The curve of $Ce_{0.50}Zr_{0.50}O_2$ mixed oxide catalyst shows the trend to be more active than the $Ce_{0.25}Zr_{0.75}O_2$.

This can be explained by the results of XRD, Raman and TPR. The summary from XRD pattern (Figure 4.2) and Raman spectra (Figure 4.10) shows that the solid solution is mainly found in $Ce_{0.75}Zr_{0.25}O_2$ and $Ce_{0.50}Zr_{0.50}O_2$ mixed oxide catalyst, respectively, and just a little amount in $Ce_{0.25}Zr_{0.75}O_2$ mixed oxide catalyst. This is the reason that why $Ce_{0.75}Zr_{0.25}O_2$ has the highest catalytic activity for CO conversion, which caused by its easiest reducible property.

TPR results (Figure 4.6 and Table 4.4) also report that $Ce_{0.75}Zr_{0.25}O_2$ is the easiest reducible catalyst followed by $Ce_{0.50}Zr_{0.50}O_2$ and $Ce_{0.25}Zr_{0.75}O_2$ mixed oxide catalyst, respectively.

In summary, $Ce_{0.75}Zr_{0.25}O_2$ mixed oxide catalyst, which the aging time equal to 120 h and calcined at 500°C, had the highest catalytic activity for CO oxidation under oxidizing condition compared to the others.

The mixed oxide catalysts, which were $Ce_{0.75}Zr_{0.25}O_2$, $Ce_{0.50}Zr_{0.50}O_2$ and $Ce_{0.25}Zr_{0.75}O_2$ those aged for 50 (Figure 4.24) and 120 h (Figure 4.25) and calcined at 500°C, were also tested in the light off temperature tests under reducing condition to compare the value of T_{50} with those done under oxidizing condition.

Figure 4.24 Light off temperature curves under reducing condition of the solid solution catalysts with the aging time = 50 h and calcined at 500°C: (♦) $Ce_{0.75}Zr_{0.25}O_2$, (■) $Ce_{0.50}Zr_{0.50}O_2$, and (▲) $Ce_{0.25}Zr_{0.75}O_2$ mixed oxide catalysts
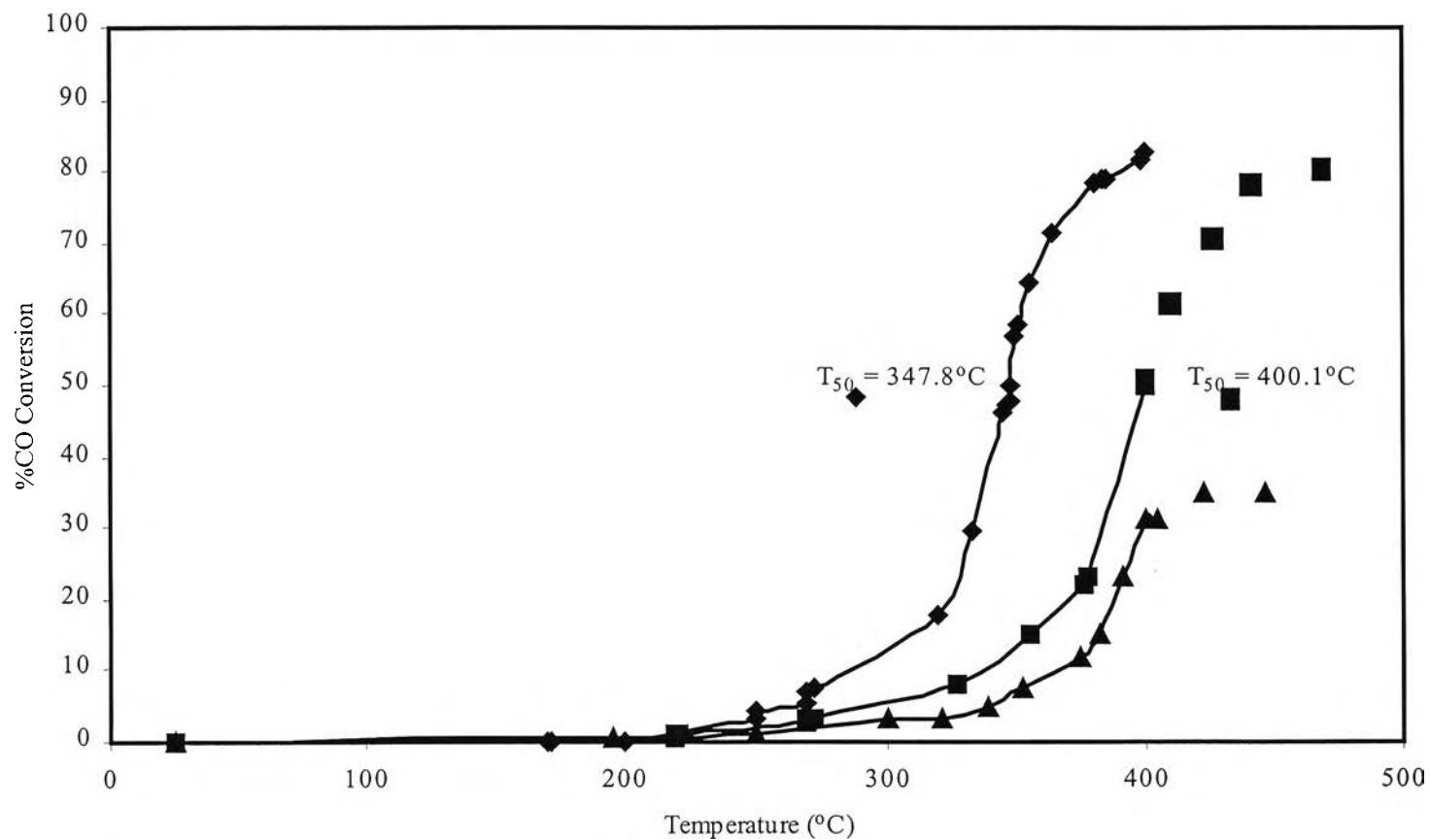
Figure 4.25 Light off temperature curves under reducing condition of the solid solution with the aging time = 120 h and calcined at $500^{\circ}C$: ($\blacklozenge$) $Ce_{0.75}Zr_{0.25}O_2$, ($\blacksquare$) $Ce_{0.50}Zr_{0.50}O_2$, and ($\blacktriangle$) $Ce_{0.25}Zr_{0.75}O_2$ mixed oxide catalysts

Besides the reactions tested under oxidizing conditions, the reactions under reducing conditions have to be tested because in the actual conditions, there may have the hydrogen in the reactions. Figure 4.24, which shows the curves of T_{50} under the reducing condition of $Ce_{0.75}Zr_{0.25}O_2$, $Ce_{0.50}Zr_{0.50}O_2$ and $Ce_{0.25}Zr_{0.75}O_2$ mixed oxide catalysts with the aging time = 50 h, was compared with Figure 4.25, which shows the curve of T_{50} of the catalysts (x = 0.25, 0.50 and 0.75) with the aging time = 120 h and calcined at 500°C.

The results show that the $Ce_{0.75}Zr_{0.25}O_2$ catalyst, which has the aging time = 50 h has the lowest T_{50} compared to other ratios, and it has lower T_{50} (336°C) than $Ce_{0.75}Zr_{0.25}O_2$ that has the aging time = 120 h (T_{50} = 348°C).

The results from XRD patterns, Raman spectra and TPR profiles can also explain the lowest T_{50} of $Ce_{0.75}Zr_{0.25}O_2$ mixed oxide catalyst as mentioned above for the tests under oxidizing condition.

The conversion of CO under reducing condition was normally less than oxidizing condition. Interestingly, in this work, when CeO_2-ZrO_2 mixed oxide catalysts were used, T_{50} under reducing condition of the samples were less than oxidizing condition, and this means the conversion of CO is higher under reducing condition (Table 4.7 compared with Table 4.9, and Table 4.8 compared with Table 4.10).

This caused from the specific property of ceria, which can promote water-gas shift reaction (Equation (4.3)).

$$CO + (\tfrac{1}{2})\, O_2 \longrightarrow CO_2 \qquad\qquad (4.1)$$

$$H_2 + (\tfrac{1}{2})\, O_2 \longrightarrow H_2O \qquad\qquad (4.2)$$

$$CO + H_2O \longrightarrow CO_2 + H_2 \qquad\qquad (4.3)$$

Under reducing condition, CO oxidation (Equation (4.1)) is occurred as same as under oxidizing condition. But, in addition, the added H_2 was reacted with O_2 to form water, which further reacted with CO in the promotion of ceria. As a result, CO conversion under reducing condition is higher than under oxidizing condition.

Table 4.7 Light off temperature (T_{50}) of catalysts prepared with the aging time = 50 h under oxidizing condition

Calcination Temperature (^{o}C)	T_{50}		
	Ce : Zr Ratio		
	75 : 25	50 : 50	25 : 75
500	356	353	*
900	*	*	*

* The sample cannot reach 50 % conversion of CO within the range of reaction temperature

Table 4.8 Light off temperature (T_{50}) of catalysts prepared with the aging time = 120 h under oxidizing condition

Calcination Temperature (^{o}C)	T_{50}		
	Ce : Zr Ratio		
	75 : 25	50 : 50	25 : 75
500	350	*	*

* The sample cannot reach 50 % conversion of CO within the range of reaction temperature

Table 4.9 Light off temperature (T_{50}) of catalysts prepared with the aging time = 50 h under reducing condition

Calcination Temperature (^{o}C)	T_{50}		
	Ce : Zr Ratio		
	75 : 25	50 : 50	25 : 75
500	336	380	134

Table 4.10 Light off temperature (T_{50}) of catalysts prepared with the aging time = 120 h under reducing condition

Calcination Temperature (°C)	T_{50}		
	Ce : Zr Ratio		
	75 : 25	50 : 50	25 : 75
500	348	400	*

* The sample cannot reach 50 % conversion of CO within the range of reaction temperature

T_{50}, the temperature giving 50 % CO conversion for all of the catalysts, was found from the figures and was tabulated in Tables 4.5 to 4.8. Lower T_{50} indicated relatively greater catalytic activity (Haruta and Sano, 1983). The natures of catalysts have an impact on the catalyst activity (Tanielyan and Augustine, 1992).

From the results, the amount of zirconia added to ceria had a seriously effect on the T_{50}. The addition of zirconium into the lattice of cerium resulted in a higher T_{50}. That meant the more zirconium was added, the less catalytic activity was achieved.